Lightcraft Impulse Measurements under Vacuum

Wolfgang O. Schall
Hans-Albert Eckel
Sebastian Walther

DLR – German Aerospace Center
Institute of Technical Physics
Pfaffenwaldring 38 – 40
D-70569 Stuttgart
Germany

August 2003

Special Report

AIR FORCE RESEARCH LABORATORY
AIR FORCE MATERIEL COMMAND
EDWARDS AIR FORCE BASE CA 93524-7048

REPORT DOCUMENTATION PAGE

1. REPORT DATE (DD-MM-YYYY) 30-09-2002	2. REPORT TYPE Special	3. DATES COVERED (From - To) 01 October 2001 – 30 September 2002
4. TITLE AND SUBTITLE **Lightcraft Impulse Measurements under Vacuum**		**5a. CONTRACT NUMBER** EOARD FA8655-02-M4017
		5b. GRANT NUMBER
		5c. PROGRAM ELEMENT NUMBER 62203F
6. AUTHOR(S) Wolfgang O. Schall; Hans-Albert Eckel; Sebastian Walther		**5d. PROJECT NUMBER** 4847
		5e. TASK NUMBER 0159
		5f. WORK UNIT NUMBER 549907
7. PERFORMING ORGANIZATION NAME(S) AND ADDRESS(ES) DLR – German Aerospace Center Institute of Technical Physics Pfaffenwaldring 38 – 40 D-70569 Stuttgart, Germany		**8. PERFORMING ORGANIZATION REPORT NO.** SPC 02-4017
9. SPONSORING / MONITORING AGENCY NAME(S) AND ADDRESS(ES) Air Force Research Laboratory (AFMC) AFRL/PRSP 10 E. Saturn Blvd. Edwards AFB CA 93524-7680		**10. SPONSOR/MONITOR'S ACRONYM(S)**
		11. SPONSOR/MONITOR'S REPORT NUMBER(S) **AFRL-PR-ED-TR-2002-0044**

12. DISTRIBUTION / AVAILABILITY STATEMENT

Approved for public release; distribution unlimited.

13. SUPPLEMENTARY NOTES

14. ABSTRACT

Under an EOARD contract, the DLR has conducted a series of comparative impulse measurements for two different lightcraft configurations with the same nozzle exit diameter of 10 cm: The German design (GL) is of the more conventional parabolical bell shape with a plasma breakdown region at the focal point of a parabola. The second lightcraft was supplied by the Air Force Research Laboratory (AFRL), and was designated as model 200-¾. The experiments utilized the DLR multi-gas laser, running in CO_2 with a laser wavelength of 10.6μm. It was the goal of this investigation to extend previous atmospheric impulse measurements to a vacuum environment and to measure specific propellant consumption of the solid propellant Delrin in order to determine the exhaust velocity and the specific impulse for both lightcrafts as a function of the laser pulse energy at various pressures.

15. SUBJECT TERMS
propulsion; lightcraft; impulse; parabola; laser; atmospheric impulse; vacuum; propellant; solid propellant; exhaust velocity; specific impulse; laser pulse energy

16. SECURITY CLASSIFICATION OF:			17. LIMITATION OF ABSTRACT	18. NUMBER OF PAGES	19a. NAME OF RESPONSIBLE PERSON Franklin B. Mead III
a. REPORT **Unclassified**	**b. ABSTRACT** **Unclassified**	**c. THIS PAGE** **Unclassified**	A	65	**19b. TELEPHONE NO** *(include area code)* (661) 275-5929

NOTICE

When U.S. Government drawings, specifications, or other data are used for any purpose other than a definitely related Government procurement operation, the fact that the Government may have formulated, furnished, or in any way supplied the said drawings, specifications, or other data, is not to be regarded by implication or otherwise, or in any way licensing the holder or any other person or corporation, or conveying any rights or permission to manufacture, use or sell any patented invention that may be related thereto.

FOREWORD
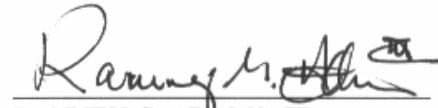
This special technical report, entitled "Lightcraft Impulse Measurements under Vacuum," presents the results of an in-house study performed under JON 48470159 by AFRL/PRSP, Edwards AFB CA. The Principal Investigator/Project Manager for the Air Force Research Laboratory was Dr. Frank Mead.

This report has been reviewed and is approved for release and distribution in accordance with the distribution statement on the cover and on the SF Form 298.

FRANKLIN B. MEAD, JR.
Project Manager

RONALD CHANNELL
Chief
Propellants Branch

PHILIP A. KESSEL
Technical Advisor
Space & Missile Division

RANNEY G. ADAMS, III
Public Affairs Director
AFRL-ERS- PAS 03-183

This Page Intentionally Left Blank

SPC 02 – 4017

Lightcraft Impulse Measurements under Vacuum

EOARD contract No. FA8655-02-M4017

Report

September 2002

Project officer: **Wolfgang O. Schall**

Co-authors: **Hans-Albert Eckel, Sebastian Walther**

DLR – German Aerospace Center
Institute of Technical Physics
Pfaffenwaldring 38 – 40
D-70569 Stuttgart
Germany

The Contractor, German Aerospace Center (DLR), Institute of Technical Physics, hereby declaress that, to the best of its knowledge and belief, the technical data delivered herewith under Contract No. FA8655-02-MA4017 is complete, accurate, and complies with all requirements of the contract.

Stuttgart, 30. September 2002

Prof. W.L. Bohn
Director
Institute of Technical Physics

I certify that there were no subject inventions to declare as defined in FAR 52.227-13, during the performance of this contact.

Stuttgart, 30. September 2002

Prof. W.L. Bohn
Director
Institute of Technical Physics

Lightcraft Impulse Measurements under Vacuum

List of figures

German Lightcraft:

1. INTRODUCTION

Under its EOARD contract No. F61775-00-WE033 (2001)[1] DLR has conducted a series of comparative impulse measurements for two different lightcraft configurations with the same nozzle exit diameter of 10 cm: The German design (GL) is of the more conventional parabolical bell shape with a plasma breakdown region at the focal point of the parabola. The second lightcraft had been supplied by the Air Force Research Laboratory (USAFRL), Whitesands, NM and was designated as model 200-3/4[2]. This US lightcraft (USL) has a configuration similar to a plug nozzle with a ring shaped plasma formation zone at the circumference of the mirror/nozzle structure. A central parabolic spike reflects the incoming light radially outward and concentrates it on a ring of solid propellant. Fig. 1 shows the two lightcrafts together with a sketch of the respective light paths.

Fig. 1a - German lightcraft

Fig. 1b - US lightcraft
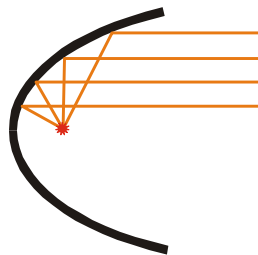
The thrust chamber of the German lightcraft is made of aluminum and is polished on the inside of the parabola. The height of the parabola is 62.5 mm and the focal distance from the vertex is 10 mm. A 2 mm thick metal pin extends about 20 mm from the vertex along the axis of the parabola through the focal point and serves as ignition pin to ensure the breakdown at the focal point for all laser pulse energies.
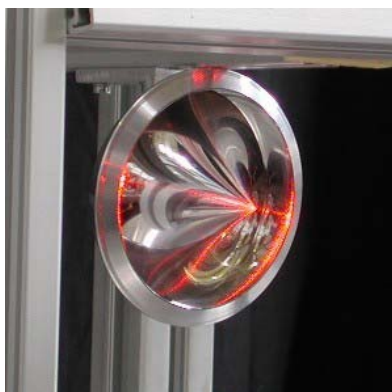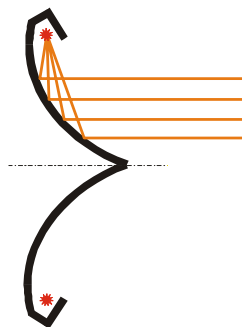
Two figures of merit characterize the performance and efficiency of pulsed laser propulsion: The impulse coupling coefficient, c_m, is the ratio of the mechanical impulse imparted on the lightcraft and the laser pulse energy. It is a measure for the velocity increase per pulse and

together with the pulse repetition frequency determines the thrust. The specific propellant consumption, μ, is the mass exhausting from the lightcraft divided by the laser pulse energy. For a solid propellant it can be easily measured by weighing the propellant before and after a certain number of laser pulses. The ratio of the two numbers yields the average nozzle exhaust velocity $v_e = c_m / μ$. Expressed as the so-called specific impulse $I_{sp} = v_e / g_0$ ($g_0 = 9.81$ m/s^2 is the Earth's gravity) the fundamental performance parameters in rocketry are determined. For instance for a non-staged flight to LEO a specific impulse of greater than 600 s is necessary. In addition, with known exhaust velocity and mass loss the kinetic energy of the exhausted jet can be calculated and the jet efficiency (ratio of the kinetic jet energy to the laser pulse energy) determined. All variables are given in SI units: c_m (N/MW = 10^{-6} N/W = 10^{-6} Ns/J); μ (μg/J = 10^{-9} g/J); I_{sp} (s).

In the previous study the impulse measurements have been performed with two different penduli in order to synchronize the results with each other. The first pendulum was used in all German measurements and corresponds to a nearly mathematical pendulum. The second pendulum was supplied by the USAFRL and was of the rigid type. All the measurements were carried out in air at atmospheric pressure. The GL used laboratory air as the only propellant. In contrast, most of the measurements with the USL used Delrin as propellant in addition to the surrounding air. Only the utilisation of this solid propellant guaranteed reproducible impulses with equal or better performance than the GL. There is a possibility that air and Delrin vapor react chemically and release additional energy. For a better comparison of the performance data of the two lightcrafts it is necessary to confirm these results with GL operating with Delrin as well. An attempt should be made to separate out a possible contribution of a chemical reaction.

The experiments utilized the DLR multi-gas laser, running in CO_2 with a laser wavelength of 10.6 μm. The typical pulse length was 10 to 12 μs. The laser can be operated with either a stable resonator, delivering a flat near field intensity distribution, or with an unstable resonator having a rectangular ring structure in the near field. Because of a better utilization of the gain medium in the laser higher laser pulse energies could be obtained with the unstable configuration. However, the experiments showed that these higher energies do not necessarily increase the imparted impulse on the lightcraft. As a

function of the laser pulse energy at least for the GL maximum impulse coupling coefficients have been found for a laser beam of the stable resonator configuration. For the USL the pulse energies with the stable resonator remained too low to reach the point of roll-over. This point was found at lower pulse energies with the unstable resonator beam. From this point on no further increase in delivered impulse was found.

The experiments of the first study were valuable with respect to the comparison of different operational and measurement conditions. In the practical application of laser propulsion they can only describe the propulsion properties in dense air. For flights to higher altitudes and into low Earth orbits (LEO) most of the propulsive process will occur outside of the atmosphere under low ambient pressure or even vacuum conditions that make the utilization of on-board carried propellant indispensable. As the flight altitude increases the atmospheric pressure decreases and the air density decreases exponentially. It is therefore essential for any projection of laser propulsion performance to measure the momentum coupling coefficient as a function of the surrounding air pressure. The utilization of a solid propellant at various pressures also allows the separation of the contributions of the two simultaneously propelled matters, air and the vapor of the solid propellant. While the cessation of air supported thrust at reduced pressures may lead to a reduction of the impulse coupling coefficient, for the increased expansion of the additional propellant into vacuum an increase of c_m can be expected. For this reason, it is impossible to predict or extend the present results to the low pressure and vacuum regime.

It was the goal of this investigation to extend the impulse measurements to a vacuum environment and, by measuring also the specific propellant consumption of the solid propellant Delrin, to determine the exhaust velocity and the specific impulse for both lightcrafts as a function of the laser pulse energy at various pressures.

2. EXPERIMENTAL SETUP

2.1 Improvements of the experimental setup
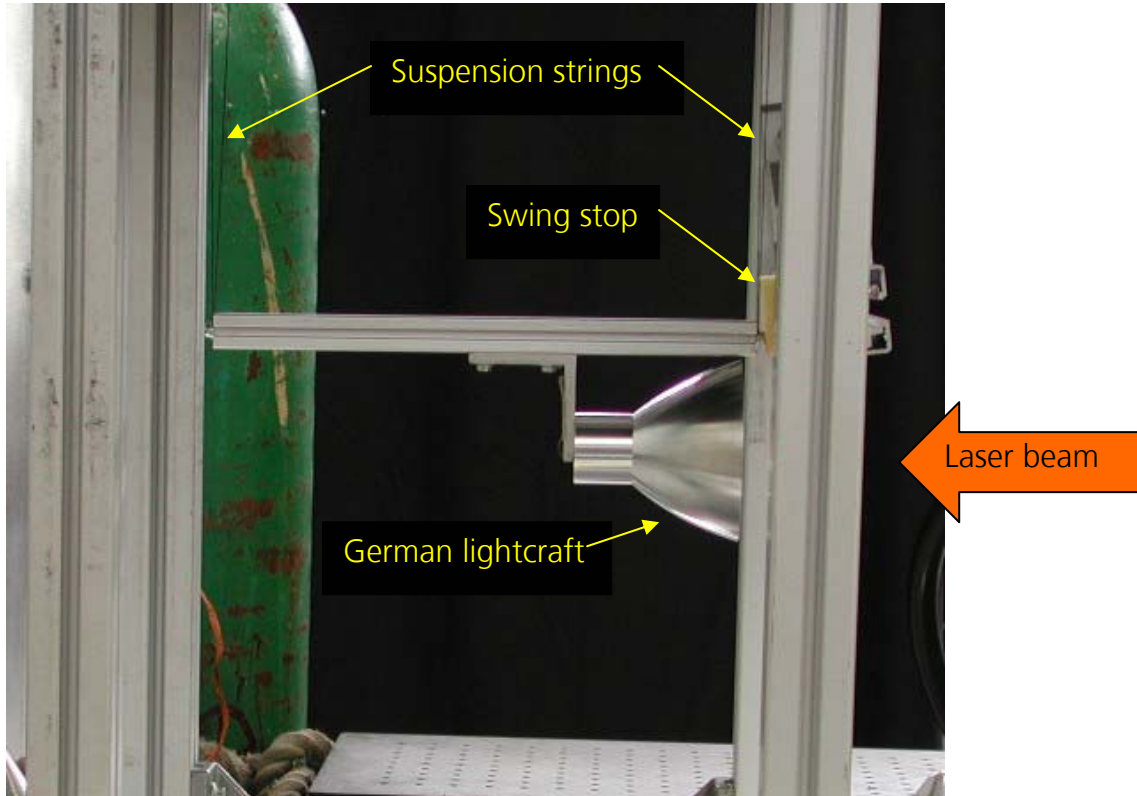
Fig. 2a - Side view of open vacuum test stand

Basically the same experimental arrangement with the vacuum vessel has been used as in the previous study. For all measurements the German pendulum type was employed, however in a slightly modified version to ease the mounting of the two lightcrafts and the repositioning after each laser pulse without opening the vacuum vessel. As Fig. 2 shows, the lightcraft was attached to a short profiled aluminum beam. This beam was fixed at the end of four strings of thin wire in a V-type arrangement. The arrangement prevented a turning motion of the lightcraft. At its rest point the beam just touched a motion stopper of soft foam rubber. This acted as strong damper of the lightcraft oscillations after each laser pulse and brought the lightcraft to a reproducible rest after only a few swings. The motion was recorded by a diode laser-based distance meter with an accuracy of the order of 1/10 of a millimeter. The impulse was calculated from the maximum displacement after the laser pulse. The length of the pendulum for the German lightcraft was 645 mm.

The laser pulse energy was also measured online by the following new method. A small hole (2 mm diameter) in the center of the metallic resonator back mirror allowed the outcoupling of a small fraction of the total laser energy. This fraction was directly measured with an energy meter. The calibration was done by comparing the signal of
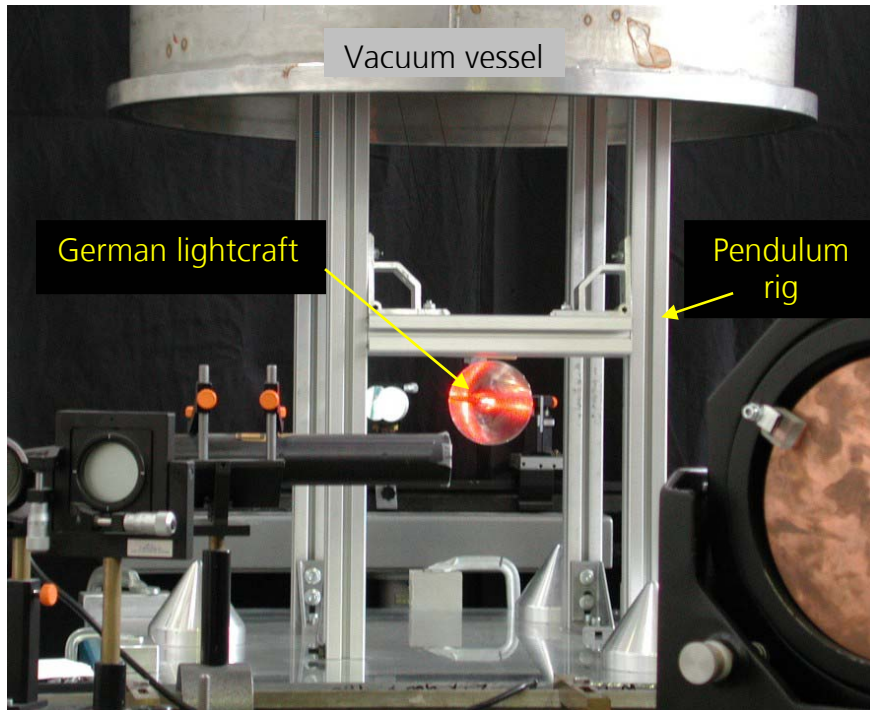
Fig. 2b - Front view of open vacuum test stand

the energy meter with the more direct measurement of the full laser beam as described in the previous report. Because of a possible power dependence of this method due to mode jumps in the resonator as the power input is increased, the calibration has been performed over the whole energy range of measurements. This procedure resulted in a linear calibration function that was entered into the computer for immediate determination of the real pulse energy. The deviation of the linear function from the actual power dependency was on the order of 1% and thus absolutely sufficient with respect to the experimental accuracy.

The vacuum vessel was connected to a pump of 65 m^3/h pumping speed. The pressure in the vessel was measured with two mechanical Wallace&Tiernan vacuum manometers, one with a pressure range of one bar for moderately reduced pressures and a second one in the range from 0 to 130 mbar, which allowed the adjustment of the pressure to

below 1 mbar. In all vacuum measurements the test was carried out, when the pressured gauge showed 1 mbar or less.

2.2 Measurement program

Of primary interest was the reduction of the impulse and the coupling coefficient, as the air pressure was reduced. This has been measured for the GL for various fixed laser pulse energies. In a further attempt the GL was equipped with the same solid propellant Delrin, as the USL has been operated with all the time. A cylindrical pin of Delrin was placed in the focal region of the lightcraft. This enabled a direct performance comparison between the two lightcraft configurations. These measurements have also been carried out at various pressure levels from 10^{-3} to 1 bar at a constant energy level. The suspicion of a chemical reaction between Delrin vapor and the surrounding air made it necessary to supplement the measurements in air by similar tests with nitrogen at various pressure levels. In all experiments with Delrin the amount of evaporated Delrin has been determined by weighing the propellant probes before and after 3 pulses of equal voltage setting of the main discharge of the laser. The voltage setting defined the pulse energy within narrow margins. Finally, the pulse energy has been varied, while keeping the pressure constant at < 1 mbar and at atmospheric pressure. During the measurements it had been noted that the intensity of the laser light on the surface of the Delrin influences amount of evaporated Delrin. Therefore, additional measurements have been made using a propellant pin of different size and also by changing the direction of irradiation on the pin.

As far as they are relevant to the USL, the foregoing experiments have been repeated with the USL; that is the influence of pressure on the performance at constant pulse energy and varying the pulse energy at vacuum condition. Again, for every parameter setting a new Delrin ring was used and weighed after every three pulses to determine the mass loss. Under vacuum condition, when no air can participate at the thrust process, it is possible to calculate from the measured numbers the exhaust velocity and the jet efficiency. Based on certain model assumptions an estimate of the air fraction in the exhaust gas, the velocity and the jet efficiency can be gained for other pressures, too.

3. RESULTS

3.1 German Lighcraft without and with Delrin

3.1.1 Dependency on pressure with air alone

The pendulum mass was found to 438.3 g by weighing and the pendulum length was 645 mm. The ignition pin was always in place. The first experiments at reduced pressure were carried out in air alone for 4 values of the pulse energy. Every parameter set was repeated at least two times.
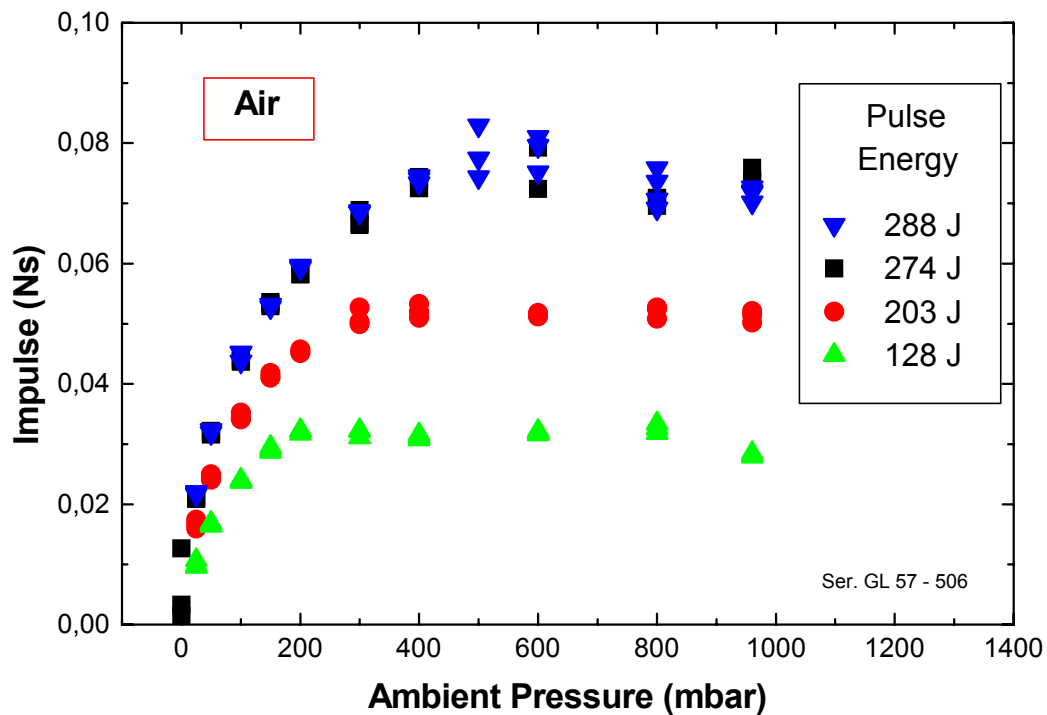
Fig. 3 - Impulse vs. pressure with air as propellant

Fig. 3 shows the result for the measured impulse as a function of the pressure in the vessel. The impulse increases strongly with the energy of the laser pulse up to a certain threshold level. However, a nearly constant value is found above the threshold pressure. The threshold pressure depends on the pulse energy and for 128 J is as low as

200 mbar. For the high pulse energies at 274 J and 288 J it is reached at 500 mbar. It is conceivable that for even higher pulse energies the threshold pressure approaches the atmospheric pressure. While the impulse above the threshold pressure is nearly constant within the accuracy of the measurement, there seems to be a weak maximum for the pulse energy of 280 J at 500 mbar.
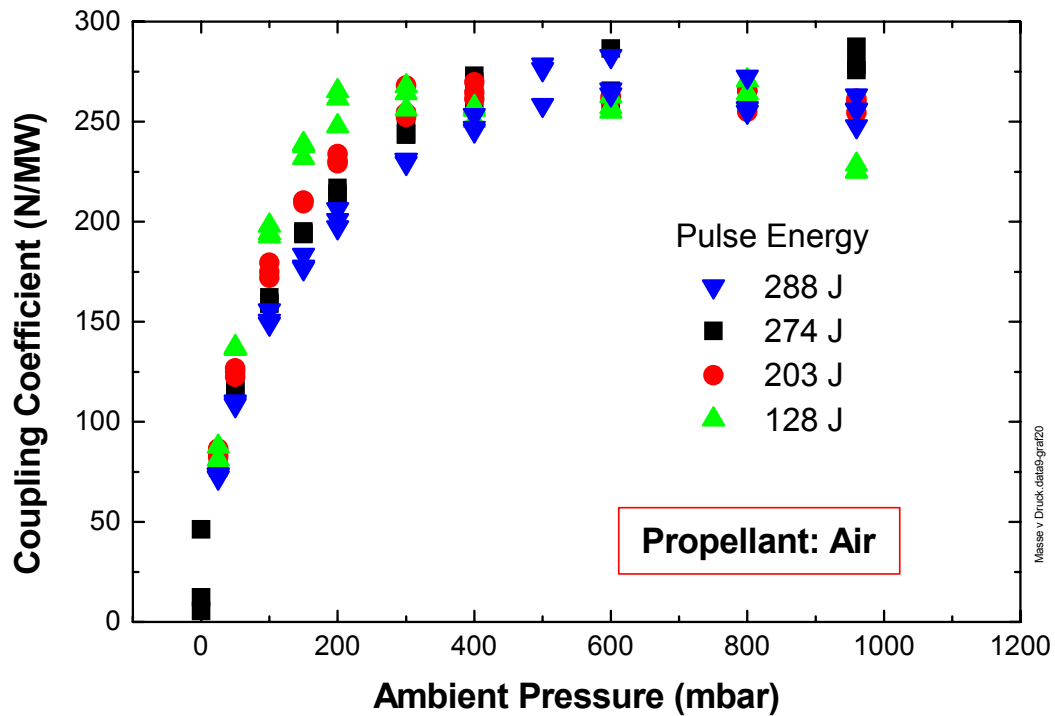
Fig. 4 - Coupling Coefficient for air and different laser pulse energies vs. ambient pressure

If the impulse coupling coefficient, c_m, is determined from these measurements by dividing the impulse by the pulse energy, the result in Fig. 4 is obtained. Now the values of the maximum coupling coefficients differ only little and amount to 250 to 280 N/MW. The low value of 225 N/MW for 128 J and 1 bar corresponds to the general decrease of c_m for lower energies (compare diagram D4 in Sec. 3.1.2.3 of ref. 1). As the pressure is reduced the curve for this pulse energy increases at first to a value of 260 to 270 N/MW. Although this behaviour has already been noted for the absolute impulse, it is not understood. A possible explanation could be that the expansion of the accelerated air goes to a lower pressure, thus reaching a higher exit velocity. This effect is later

countered by the reduction of the exhausted air mass in such a way that initially a nearly balanced situation occurs.

The operation with very low pressures was accompanied by a notable thermal load in the vertex region of the paraboloid. A yellowish colouring of the aluminum surface could be seen, indicating the appearance of high temperatures.

3.1.2 Dependency on pressure with Delrin added

Delrin as an additional propellant has been placed in the focal region of the parabolic thruster mirror. For this purpose Delrin cylinders of 15 mm in length and 8 mm in diameter were stuck on the ignition pin and pushed to vertex of the paraboloid (Fig. 5). The light was thus concentrated radially on the cylinder walls with a certain lateral intensity distribution. A new pin was attached for every new parameter set and hence after three pulses. It was repetitively observed that the second impulse out of several on the same target pin was higher than the first and the third. Each pin was weighed before and after use in order to find the mass loss, m, for the applied laser pulse energy, E. By this the specific propellant consumption $\mu = m / E$ could be determined. Fig. 6 shows an example of a used pin. The groove from the evaporated material follows in its shape approximately the intensity distribution on the cylinder wall.

Fig. 5 - Delrin pin inside GL

Fig. 6 - Used pin

Fig. 7 summarizes the results of the impulse for pulse energies of 252 ± 10 J for the following 3 different cases: For reference, the black squares represent the already

displayed behaviour for air as the only propellant. At pressures below 2 mbar the impulse is zero. However, with Delrin an impulse of 0.06 Ns has been measured with a scatter of ± 0.005 Ns (red dots). This value corresponds to 80 % of the maximum impulse with air alone. As the air pressure is increased in steps to atmospheric pressure the impulse curve also increases linearly to the same pressure value, where the air curve
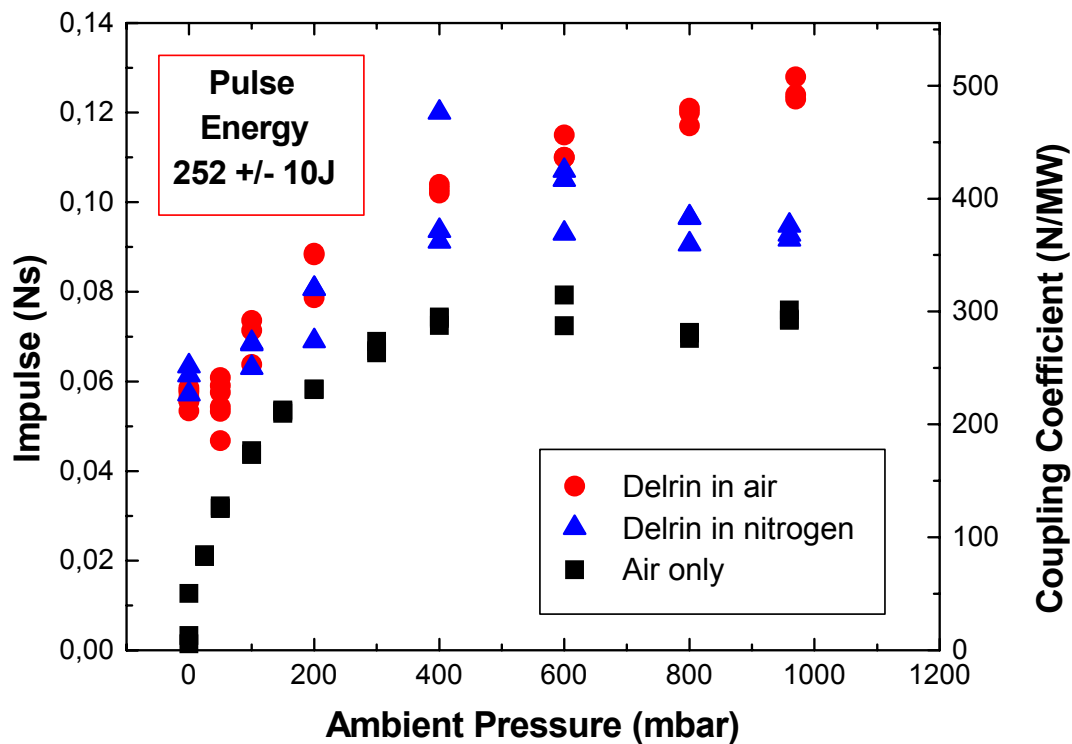
Fig. 7 - Impulse and momentum coupling coefficient for 3 propellant combinations vs. ambient pressure

begins to level off. In the range between 100 and 300 mbar the rate of increase of the Delrin curve is about the same as of the air curve. Surprisingly, from the saturation pressure of the air curve on, the Delrin curve continues to rise linearly, although with a different rate. There seems to be no indication of a saturation even at atmospheric pressure. This latter behaviour can only be explained either if more Delrin vapour is produced with increasing air pressure, or the Delrin vapour absorbs more energy that is transformed into kinetic energy, or a combustion reaction of the vapour with the air takes place, that adds energy to the gas. The latter explanation is the most likely one, because such a reaction would become stronger with the increasing availability of oxygen at rising pressure. Furthermore, in video recordings of the laser pulse interaction with the US lightcraft a flame has been seen developing in front of the lightcraft exit.

15

This is shown in a sequence of three successive video frames in Fig. 8. For the German lightcraft such a combustion must occur at least to some extend in the inside of the thruster. Otherwise the reaction energy could not contribute anymore to the impulse.
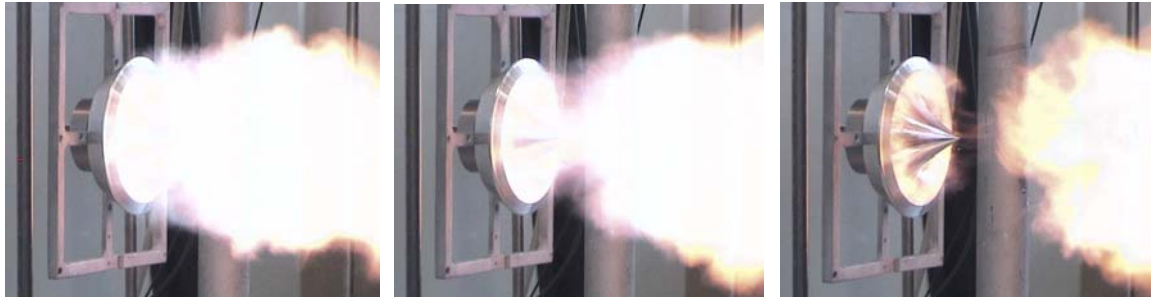
Fig. 8 - Three successive frames of a movie, showing the combustion of Delrin with the USL.

This interpretation has been checked by suppressing a possible combustion reaction in a chemically inert nitrogen atmosphere. The result is displayed in Fig. 7 as blue triangles. Up to the saturation point in air at 400 mbar the nitrogen (+ Delrin) curve coincides with the air (+ Delrin) curve. But from this pressure on the impulse in nitrogen saturates also, obviously because no energy is provided by combustion. The increase of the impulse with added Delrin over air alone amounts to 16 – 20 % and reaches 0.095 Ns instead of 0.073 Ns. However, another 0.032 Ns are added to this value by the chemical reaction energy. With this behaviour a hybrid operation has been demonstrated incidently, with 1/3 of the impulse coming from a different energy source.

The fact that the combustion process takes place in the vapor phase of the Delrin and is not a reaction on the surface of the solid can be proven by the mass loss. For a surface reaction it is expected that the mass loss would increase with the air pressure. As Fig. 9 shows that, except for the measurement at 0 mbar, the mass loss is independent of the ambient pressure. For the notably higher values at full vacuum (22 mg per pulse in the average) no explanation can be given. The mass loss is also independent of the surrounding gas and amounts to 15 mg per pulse. This is equivalent to an average specific propellant consumption of 60 µg/J.

Because in these experiments the pulse energy remained constant within the natural bandwidth of the laser, the coupling coefficient must show exactly the same behaviour

as the absolute impulse (Fig. 7 right scale). The numbers are 240 ± 25 N/MW for Delrin at vacuum, 270 N/MW for air alone at 1 bar, 370 N/MW for Delrin in nitrogen at 1 bar, and 525 N/MW for Delrin in air at 1 bar.
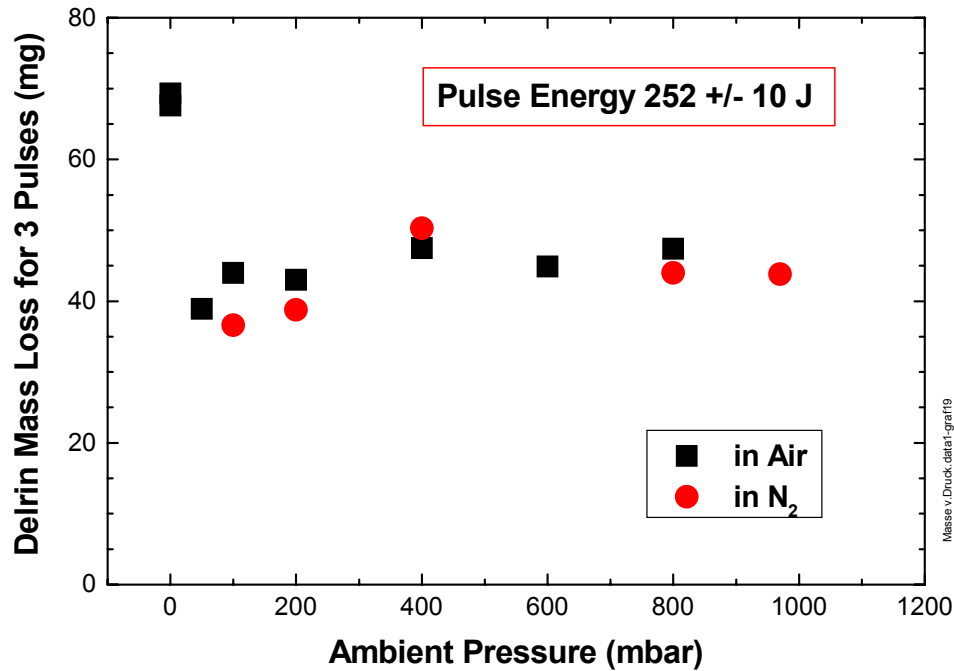
Fig. 9 - Mass loss for 3 laser pulses vs. ambient pressure of air or nitrogen

As has been stated in Sec. 1, the knowledge of both, the coupling coefficient, c_m, and the specific propellant consumption, μ, allows the direct determination of the mean effective exhaust velocity, v_j. This determination, however, is only meaningful for the vacuum case, where solely the measured Delrin mass, but no air, is exhausted. The effective exhaust or jet velocity is found to be 2.55 ± 0.1 km/s (3.74 km/s). The number is related to the higher mass loss of Delrin of 22 mg at $p = 0$ mbar. This mass loss has been confirmed later on for the measurements with variable pulse energy (Sec. 3.1.3) and are thus the more conservative data. The number in brackets is for a mass loss that corresponds to the average value of 15 mg, as found for pressures > 0 mbar.

If the jet velocity is known then the kinetic jet efficiency, η, can also be calculated. In vacuum it is 0.3 ± 0.03 (0.45). If another 30 % of energy are lost to the wall, as has been found in very early experiments from measuring the temperature increase of the

wall[3], then a remainder of 40 % (25 %) is still contained in the jet as inner energy (sensible heat and excitation) that could not be transformed to kinetic energy during the expansion process. Again, the numbers in brackets refer to the lower mass loss.

Since the amount of air that is exhausted at the various pressures is a priori unknown, it is not possible to calculate the common exhaust velocity as a function of the pressure. However, if one assumes that the efficiency of the energy deposition process is independent of the mixture ratio and no additional energy is liberated by combustion, as is the case for nitrogen, then both, the common exhaust velocity, v_c, and the mass ratio between air (index A) and Delrin vapour (index D) can be estimated. In this special case, the produced kinetic energy in the Delrin vapour under vacuum condition must be the same as in the mixture of the masses m_D and m_A that are exhausted with v_c :

$$m_D \, v_D^{\,2} \; = \; 2 \, \eta \, E \; = \; (\, m_D + m_A \,) \, v_c^{\,2}$$

From the measurements is known the ratio of the impulse in vacuum to that at some pressure:

$$W \; = \; (\, m_D \, v_D \,) \, / \, [(\, m_D + m_A \,) \, v_c \,]$$

From these two equations follows the common velocity

$$v_c = W \, v_D$$

and the mass ratio

$$m_A \, / \, m_D \; = \; \mu_A \, / \, \mu_D \; = \; 1 \, / \, W^2 \, - \, 1 \; .$$

The pressure dependence of the common exhaust velocity is shown in Fig. 10.

The velocity drops rapidly to 1.35 km/s at 400 mbar as the amount of exhausted air increases. While in nitrogen the velocity slightly increases again to 1.5 km/s at 1 bar, it drops for air to 1.2 km/s. (As before, the numbers are related to the more conservative mass loss of Delrin measured at p = 0 mbar). The different behaviour must be an artifact since the combustion effect could not be considered in the above formalism and hence the effective efficiency has changed. This becomes even more noticeable in the calculation of the mass ratio air to Delrin, as shown in Fig. 11. With increasing pressure the ratio grows from 0 to 2.2 at 400 mbar, where the curves begin to separate strongly. The ratio drops again down to 1.65 for nitrogen at 1 bar, which is correct, and grows at the same time to 3.7 for air. Since 15 mg of Delrin are exhausted independent of the pressure, due to the mass ratio of to 2.2 at 400 mbar the mass of air or nitrogen corresponds 33 mg. This is roughly 30 % of the air contained in the volume of the thruster and is consistent with derivations from other measurements.
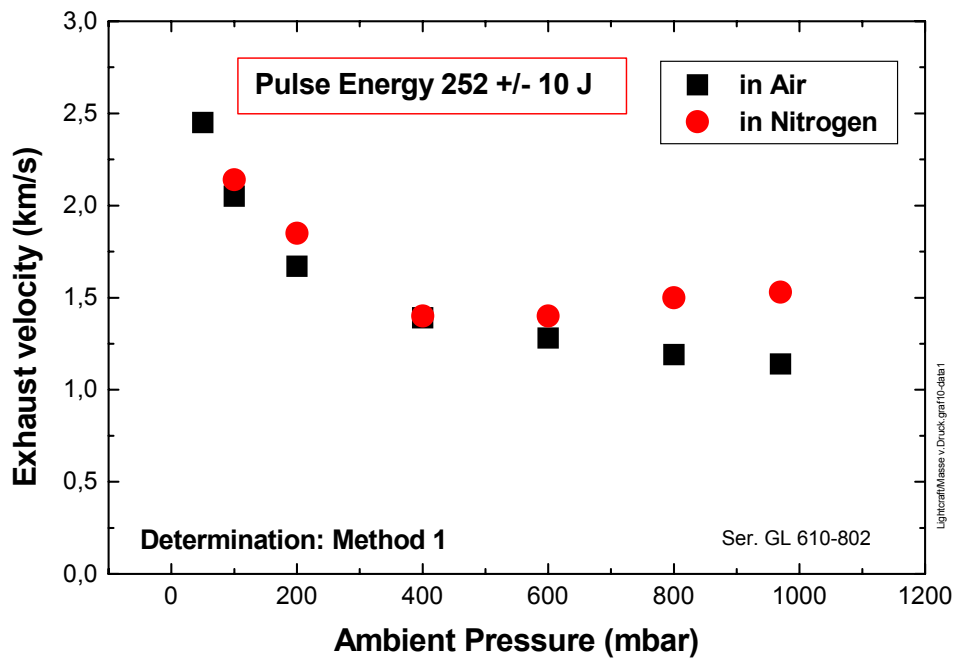
Fig. 10 - Average exhaust velocity for air and nitrogen as propellants vs. pressure, determined according to method 1
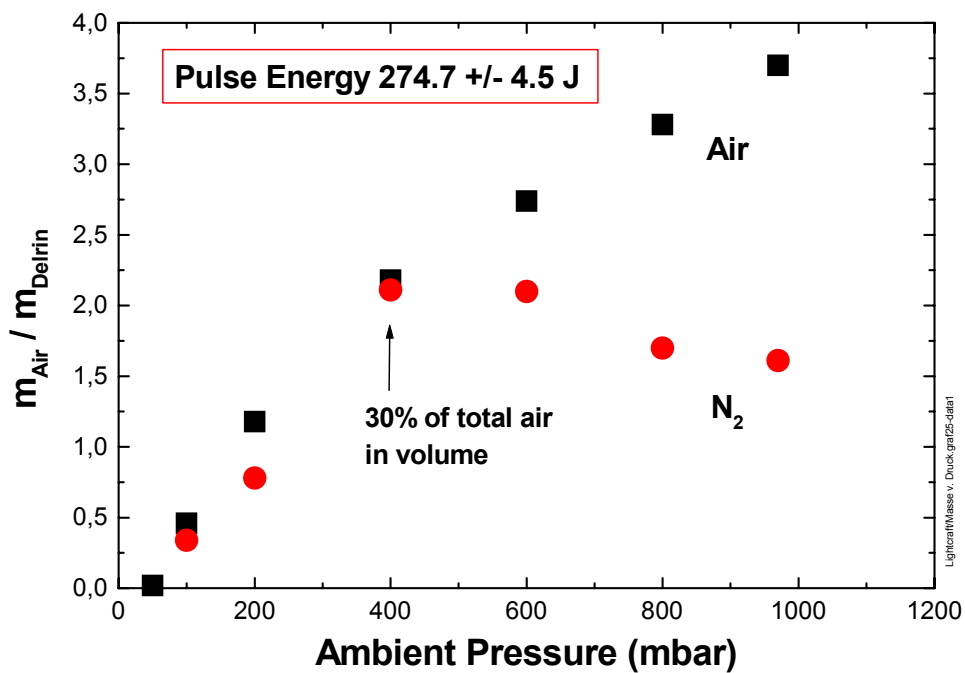
Fig. 11 - Ratio of air to Delrin for the GL vs. pressure (evaluation method 1)

The assumption of equal efficiency is doubtful for air at pressures $\geq$ 400 mbar, where the combustion energy acts as if the efficiency of the laser interaction would increase by an amount α. With an assumption of $\eta + \alpha$ a new derivation is possible. Let I_D, I_N, I_A be the measured absolute impulse values for Delrin, Delrin + nitrogen and Delrin + air, respectively, and with the same indices the exhaust velocity, v. For the exhausted gas mass we have to introduce another assumption, namely that the exhausted gas mass is the same for nitrogen and for air, $m_g = m_N = m_A$, irrespective of a different energy production and neglecting the small difference in molecular weight. The following equations can be set up from the definition of the momentum and the balance of energy:

$$v_D = I_D / m_D$$

$$2\,\eta\,E = I_D\,v_D \qquad \Rightarrow \qquad \eta = I_D\,v_D / 2\,E$$

$$2\,\eta\,E = I_N\,v_N \qquad \Rightarrow \qquad v_N = 2\,\eta\,E / I_N$$

$$2\,(\eta + \alpha)\,E = I_A\,v_A$$

$$I_N = (m_D + m_g)\,v_N \qquad \Rightarrow \qquad m_g = I_N / v_N - m_D$$

$$I_N / I_A = W_{NA} = I_N / (m_D + m_g)\,v_A$$

$$\qquad \Rightarrow \qquad v_A = I_N / (m_D + m_g)\,W_{NA}$$

$$\qquad \Rightarrow \qquad \alpha = I_A\,v_A / 2\,E - \eta$$

The new result for the velocities v_N and v_A is given in Fig. 12 for both values of the Delrin mass loss. Similarly, the mass ratio m_g / m_D, and the combustion efficiency term α are shown in Fig. 13. The values are calculated only for the mean values of the impulses and the masses. While the exhaust velocity of nitrogen continues to drop as the pressure is raised to 1 bar, the exhaust velocity of air goes up again for pressures of 400 mbar and higher. This is in fact expected as being the consequence of an additional heating by the chemical reaction. In contrast to the earlier assumption, the exhausted mass fraction of either nitrogen or air rises steeply in the low pressure regime and becomes constant in the high pressure regime because the impulse with nitrogen has saturated. In this regime the combustion efficiency term α grows to 24 % (35 %) at the pressure of 1 bar.
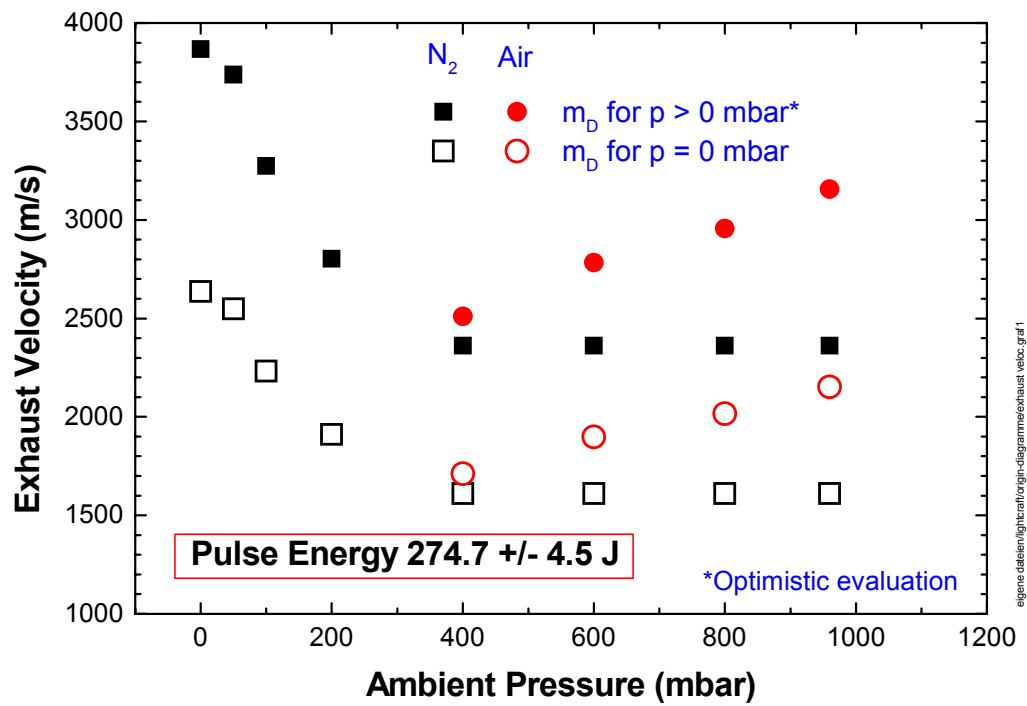
Fig. 12 - Average exhaust velocity according to the second evaluation method
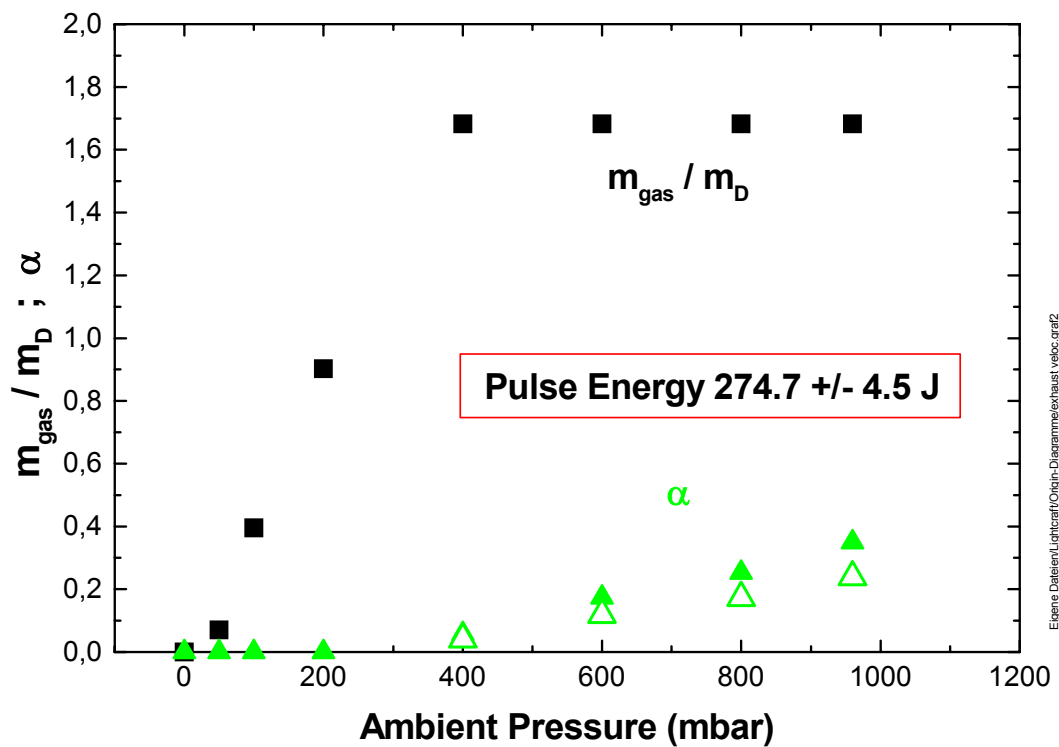
Note, that both considerations rely on some extreme assumptions and do not describe the reality in a correct way, because one number is missing, i.e. the fraction of the combustion energy. The combustion energy only manifests itself in the increase of the impulse. The reality is certainly found somewhere in between of the results from the two models. Hence, at atmospheric pressure the numbers are to expected in the range as given in the following table for air (E = 258.7 J)

Assumption	1st method $\eta N = \eta A$	2nd method $mN = mA$
vA (m/s)	1180	2150
mA (mg)	85.4	37.0
ηA (+ α)	0.30	0.54

The values for nitrogen are the same for both methods: v_N = 1590 m/s and m_N = 37 mg.

3.1.3 Dependency on the pulse energy in vacuum and atmospheric pressure
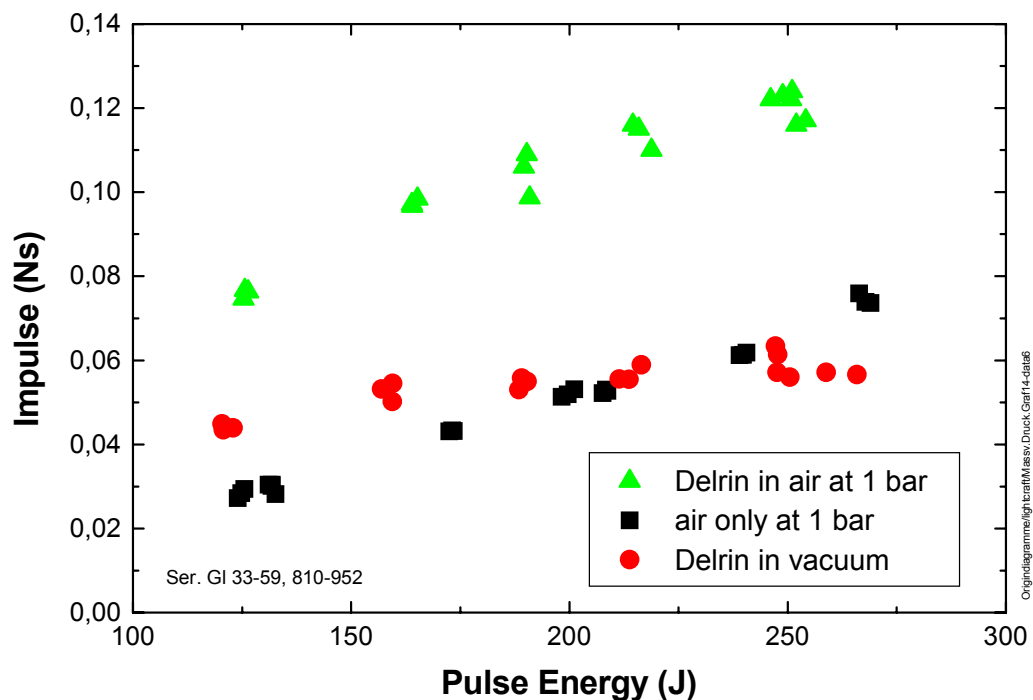
Fig. 14 - Lightcraft impulse vs. laser pulse energy for 3 cases with and without Delrin as additional propellant

Fig. 14 shows the measured impulse as a function of the laser pulse energy for 3 cases: The black squares represent the impulse at a pressure of 1 bar, when air is the only propellant. In comparison, the green triangles show the result when Delrin is added as a second propellant. While the impulse in air alone grows linearly with the pulse energy and achieves a maximum value 0.083 Ns for 251 J the values with Delrin at first grow more rapidly, but then begin to saturate for the highest energies. The maximum achieved value is 0.12 Ns and thus 50 % higher then without Delrin. If the air is now omitted by operating in vacuum (red circles), a dependency is found with a much slower growth and a fairly early saturation. Although for 126 J the impulse is still higher than with atmospheric air (0.045 Ns), at the maximum energy of 251 J it ends up lower than air (0.06 Ns).
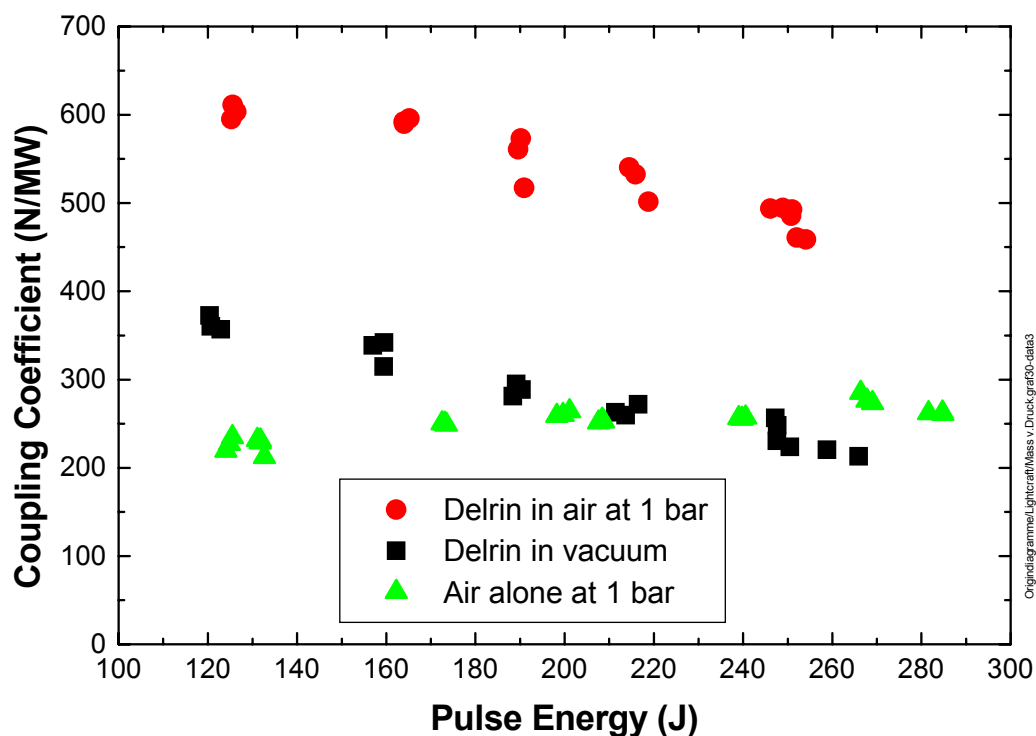
Fig. 15 - Momentum coupling coefficient vs. laser pulse energy for 3 cases with and without Delrin as additional propellant

Because the rise of the impulse is slower than the energy increase, the coupling coefficient must fall in all cases where Delrin is applied. This is indeed so, as Fig. 15 shows. The decrease for cases with Delrin is comparable and linear, only at a different level. Now the highest coupling coefficients are found for the lowest pulse energies. The

maximum values are roughly 400 N/MW for Delrin in vacuum and 650 N/MW at p = 1 bar. In atmospheric air alone there is a slight increase for low energies with a rapid saturation at about 275 N/MW. Some mechanism seems to prevent the deposition of the full energy into the Delrin. Such a mechanism could be plasma absorption in a laser supported detonation wave (LSD-wave) running towards the laser beam, that does not interact with the thruster walls to produce thrust. Or, the index of refraction changes in the shock wave front that emanates from the breakdown plasma and reduces the focal intensity by bending the light away from the focal point. The created Delrin vapour, on the other hand, seems to be transparent to the incoming light, because an absorption would raise the enthalpy of the vapor and result in a higher expansion velocity. The consequence would be a higher measured impulse. The fact that the process is more efficient when the thrust is actually lower requires a higher repetition rate of the laser if the same propulsion power is to be obtained.
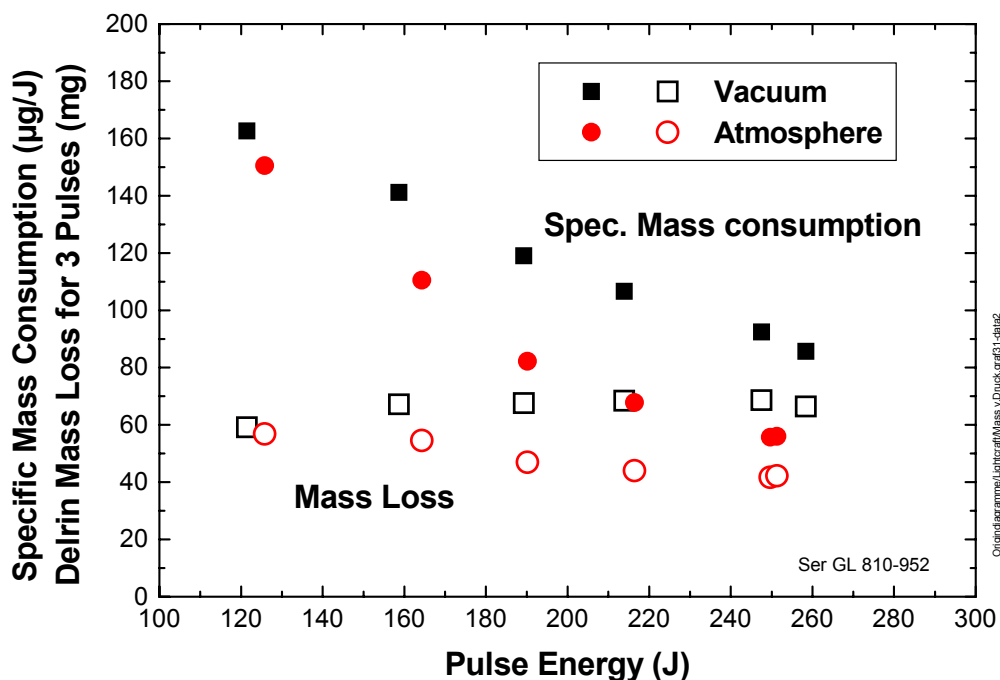
Fig. 16 - Mass loss of Delrin for 3 laser pulses (open symbols) and specific propellant consumption (full symbols) vs. pulse energy for 3 cases.

Of particular interest is now the result for the mass loss of Delrin. This is shown in Fig. 16. It is found that the mass loss is nearly independent of the pulse energy. In atmospheric air it even slightly decreases with increasing pulse energy. Consequently,

the specific mass consumption must decrease inversely proportional to the pulse energy. A possible explanation is again the creation of an LSD-wave, a travelling plasma zone that absorbs all the subsequently delivered energy.

Due to the similar decrease of both c_m and μ with increasing energy, the ratio between the two quantities, expressing the exhaust velocity, stays nearly constant. For the vacuum condition the exhaust velocity, v, can be determined directly and without any further assumption. With increasing pulse energy the exhaust velocity goes up from 2.25 km/s to 2.65 km/s only (see Fig. 24 Sec. 3.1.4). The calculation for the Delrin / air mixture according to method 1 (equal jet efficiency for operation with and without Delrin) yields a velocity of 1.3 km/s, which is within experimental error constant over the energy range. The jet efficiency, η, however decreases with increasing energy from 43 % at 125 J down to about 30 % at 250 J (Fig. 25 Sec. 3.1.4). The fraction of exhausted air to Delrin vapor, m_A/m_D, increases from 2 to 3.5 over the same range (Fig. 17). The additional energy seems to end up only in the air. A more ideal propellant should absorb all the energy in the vapor. The derived numbers for air (v, η, and m_A/m_D) are approximations within the limits of method 1. Since the corresponding dependence in nitrogen has not been measured, the other limit cannot be calculated.
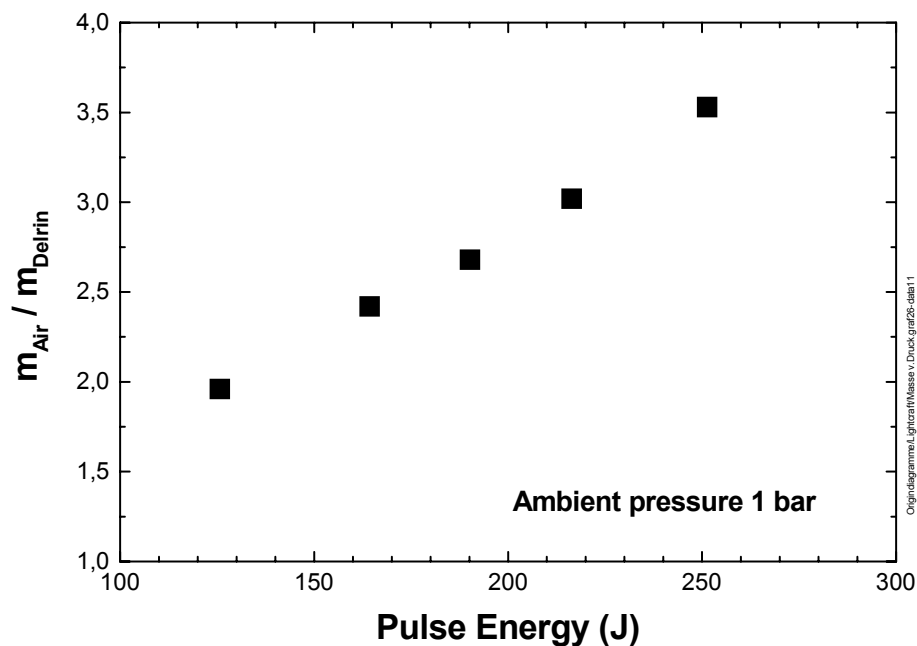
Fig. 17 - Mass ratio of air to Delrin vapor at atmospheric pressure

3.1.4 Dependency on the intensity at the Delrin surface.

Sine there is an obvious blocking of the energy delivered to the target, a lower intensity distribution at the target surface may lead to different results. The simplest way to decrease the energy distribution was to enlarge the diameter of the Delrin pin, for instance from 8 to 10 mm. This reduces the fluence level on the surface by a factor of 0.65. For a 100 J pulse the peak intensity would go down from $3 \cdot 10^7$ W/cm^2 to $1.9 \cdot 10^7$ W/cm^2 (for comparison the peak intensity on the ignition needle is $7.3 \cdot 10^8$ W/cm^2). Associated with the reduction in intensity was an enlargement of the irradiated area.
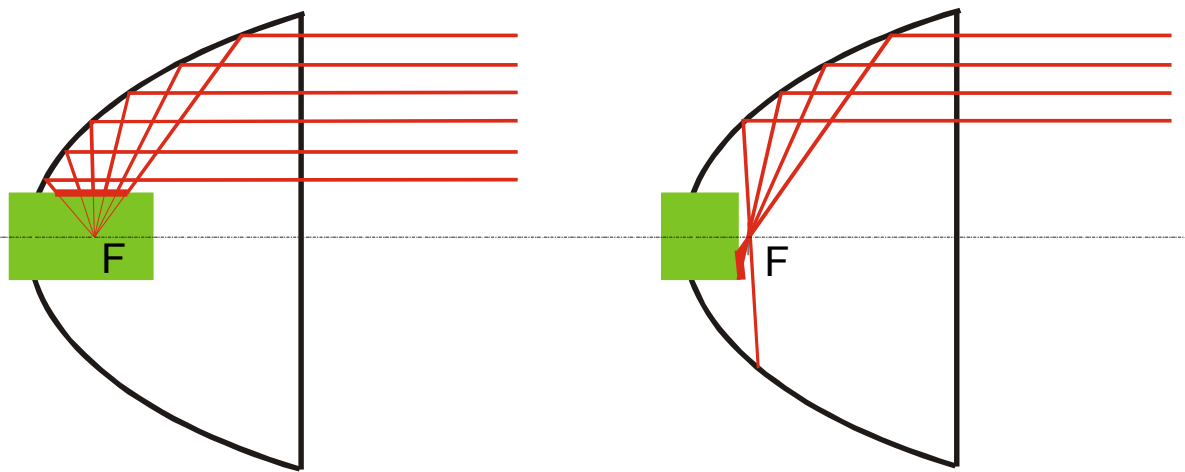
Fig. 18 - Schematic of irradiation on pin (green) side-on (left) and front-on (right)

A second test has been made going in the opposite direction: The 8 mm diameter pin was shortened to a length of 8.5 mm. In this case the light was focused on the circular front side of the cylinder with a several times higher fluence level than for the cylinder circumference of the same diameter. The two possibilities for the target irradiation are shown schematically in Fig. 18. As this figure shows, not all of the incoming light for the front side irradiation is actually concentrated on the surface. There was a second purpose for this experiment. In the case of radial irradiation the produced Delrin also expands radially. However, the thruster walls enforce an overall axial flow. Thus by turning the flow the propulsive force acts primarily against the thruster walls. In the case of the front side irradiation the Delrin vapor expands primarily in the axial direction and the thrust acts at first on the pin surface itself. This could simulate the mechanics of a direct ablation plasma thruster. Because the produced impulse on the lightcraft was so poor and because the pin was pressed on the needle so firmly by the high force that it

was difficult to remove and replace it, these experiments were only carried out for one value of the pulse energy.

The results for all experiments with a different pin size are displayed in the following figures. In addition to showing the absolute impulse of the 8 mm pin the impulse for the 10 mm pin and the impulse for the front side irradiation are displayed in Fig. 19 also.
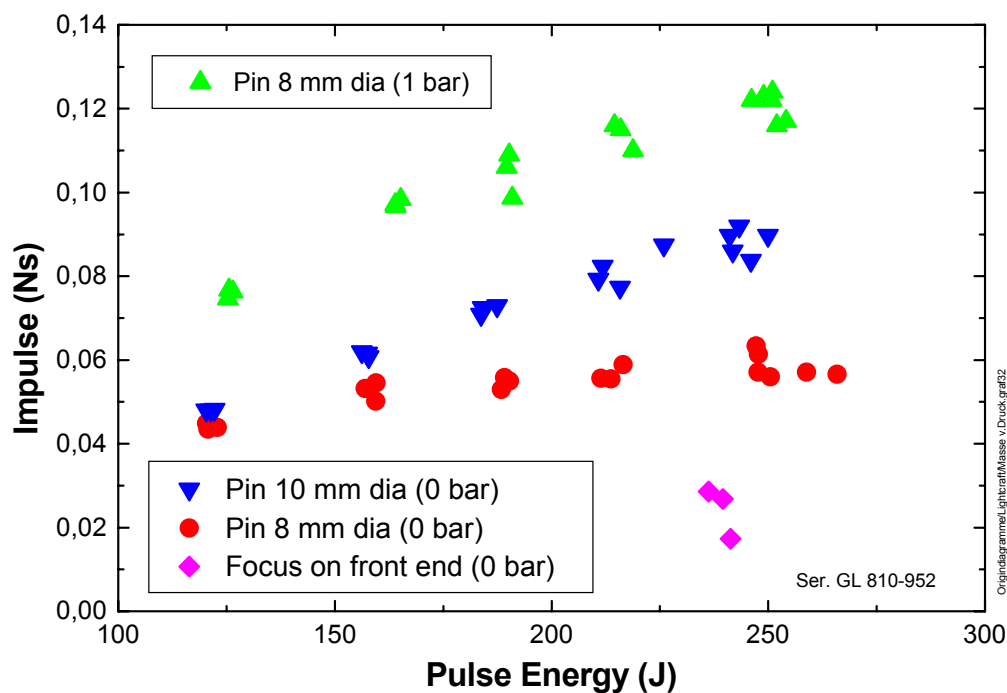
Fig. 19 - Impulse for different Delrin pin sizes and different irradiation vs. laser pulse energy

Although starting at nearly the same value at the low energies the impulse for the 10 mm pin increases significantly faster than the impulse for the 8 mm pin. At the maximum pulse energy it ends up with a 50 % higher value. This corresponds to the fact that also more Delrin mass has been vaporized (Fig. 20). In contrast, the vaporized mass in the case of the front side irradiation amounts to only 40 % of the side wall irradiation value. If now the impulse is plotted versus the evaporated mass a completely proportional relationship is found (Fig. 21). This means that the increase in impulse for higher laser pulse energies is only due to the increased in exhausted Delrin vapor mass. The Delrin vapor does not absorb any additional energy and therefore the exhaust velocity cannot increase as desired. So, the specific impulse is practically fixed.
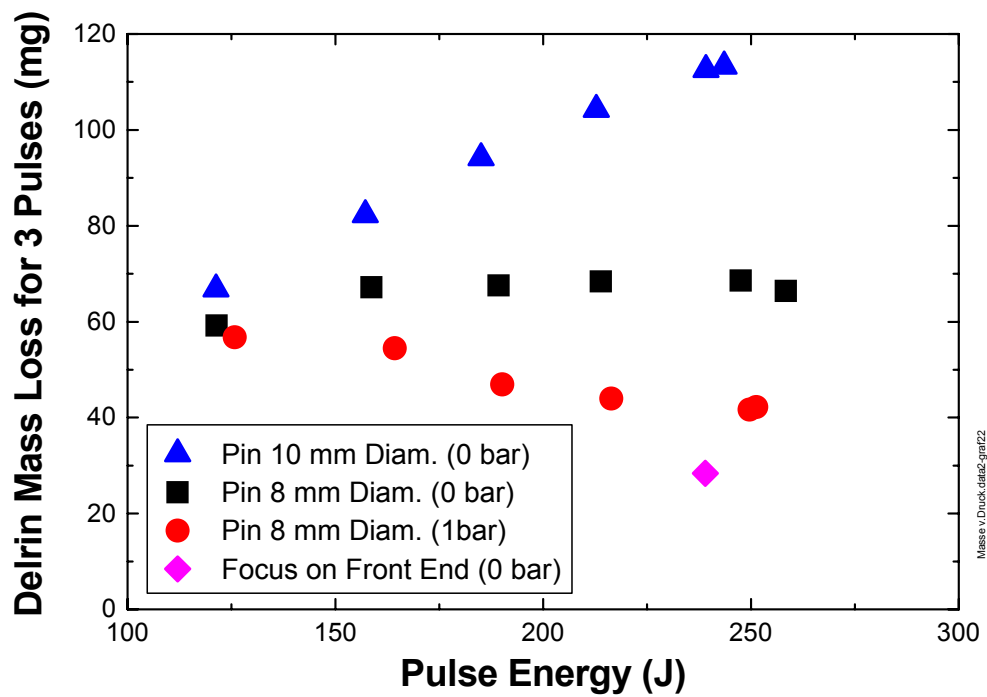
Fig. 20 - Mass loss for 3 pulses for different pin irradiations vs. laser pulse energy
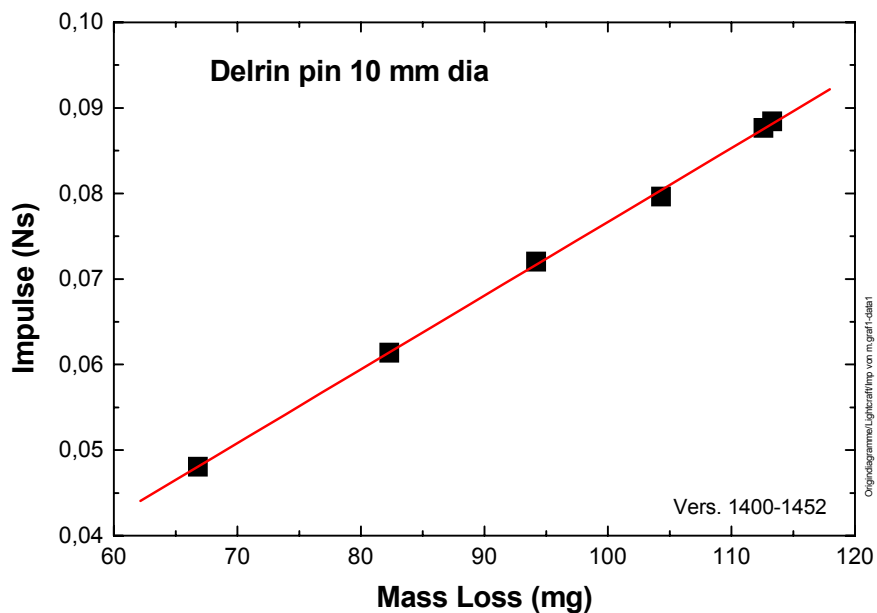
Fig. 21 - Impulse vs. mass loss

If the energy specific quantities, the coupling coefficient c_m and the specific mass consumption are derived, it is found that for the thicker pin c_m decreases much less with increasing energy than for the 8 mm pin (Fig. 22): From 420 N/MW to 370 N/MW,

corresponding to 12 % as compared to 44 % (390 N/MW to 220 N/MW). In the same manner, the specific propellant consumption decreases much less for 10 mm pin compared to the 8 mm pin (Fig. 23). The values are 195 µg/J for the lowest energy and 158 µg/J for the highest. As expected the exhaust velocities show comparably little differences. Starting from about 2.2 km/s they increase to 2.6 km/s for the 8 mm pin and to 2.35 km/s for the 10 mm pin (Fig. 24). The velocity value for the front side irradiation is similar to that of the 8 mm pin. The jet efficiency also decreases only marginally (Fig. 25) from 42 % to 37 % (compared to 43 % and 28 % for the 8 mm pin).
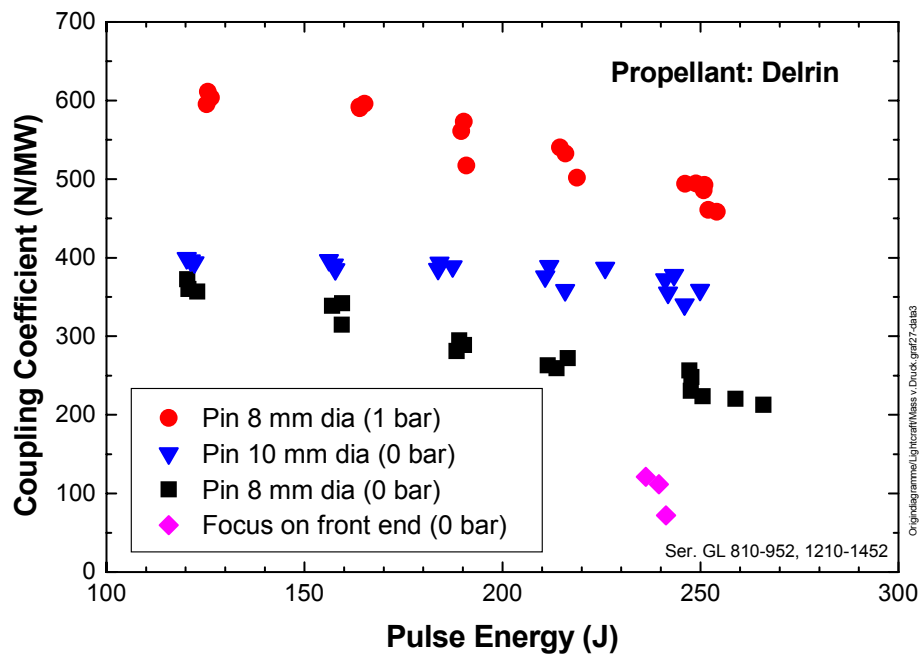
Fig. 22 - Momentum coupling coefficient for different Delrin pins vs. laser pulse energy
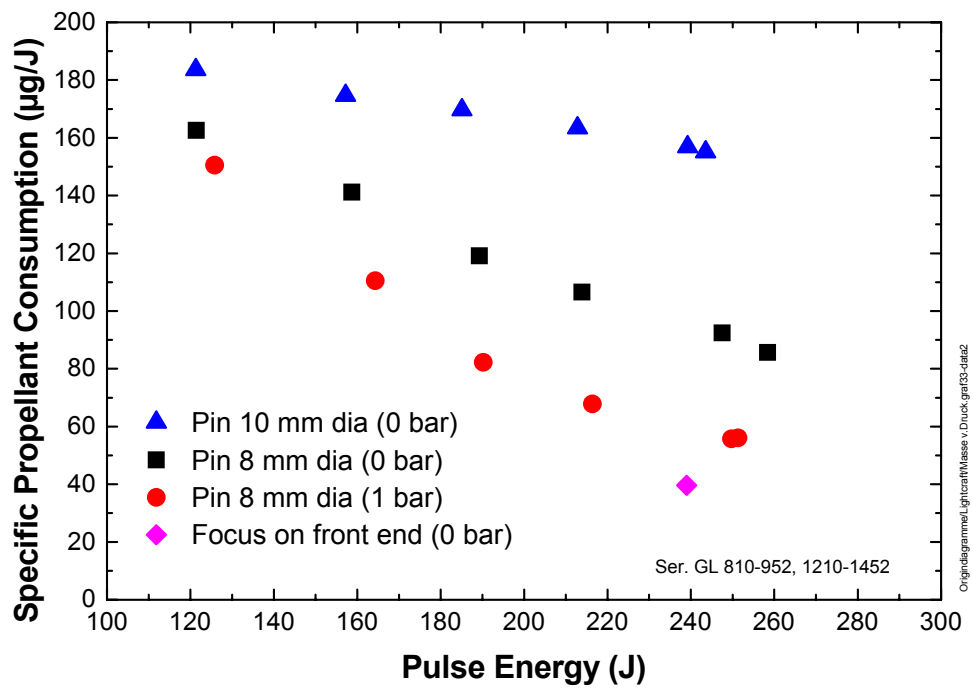
Fig. 23 - Specific propellant consumption for different Delrin pins vs. laser pulse energy
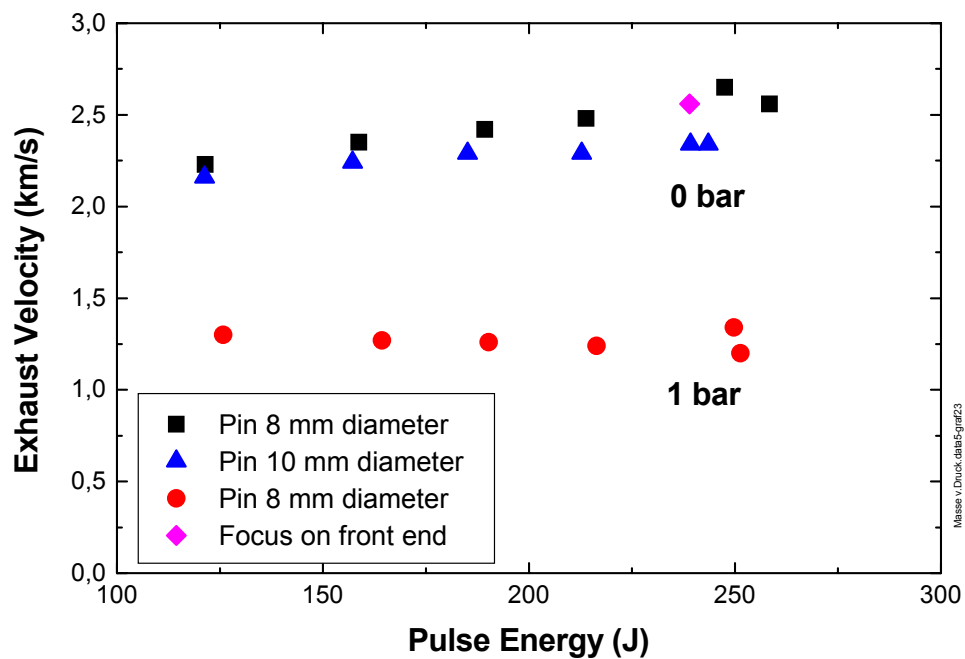
Fig. 24 - Average exhaust velocity for different Delrin pins vs. laser pulse energy
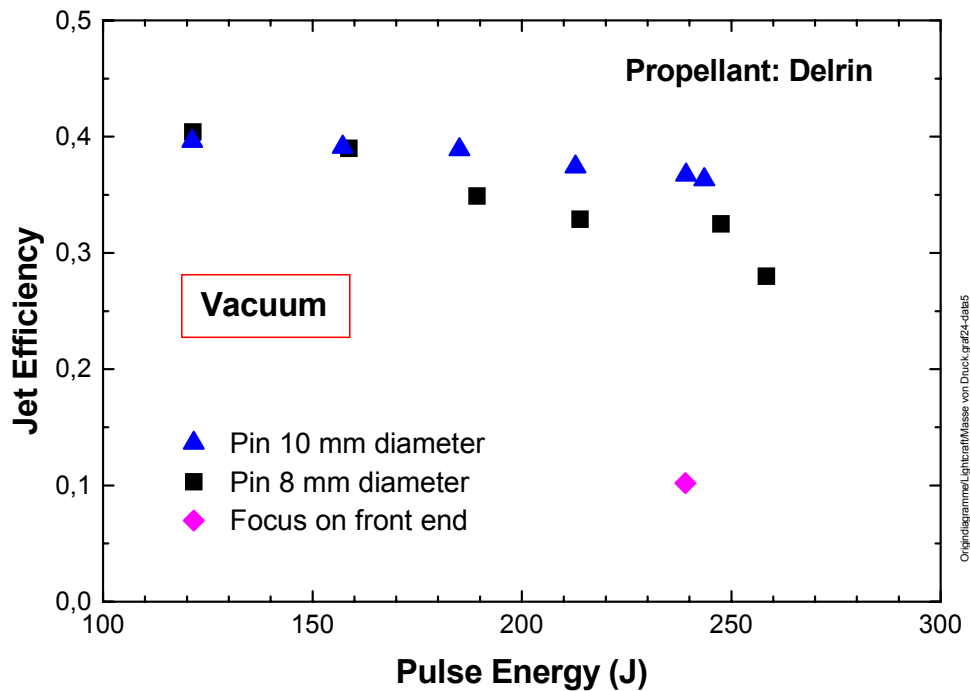
Fig. 25 - Jet efficiency for different Delrin propellant pins in vacuum vs. laser pulse energy

3.2 US-Lightcraft

3.2.1 Dependency on the ambient pressure

Leaving everything else unchanged the GL has been exchanged for the USL. The pendulum mass was 494 g and the pendulum length 645 mm. In this series the pulse energy was kept constant during the change of the ambient pressure in the vessel. The pressure was changed from below 1 mbar in several steps to approx. 970 mbar (local pressure for the open vessel). In contrast to the GL, the measurements have been carried out only with the additional propellant Delrin, since measurements in air alone did not result in reproducible and meaningful impulses with the stable resonator. The Delrin ring was exchanged after every 3 pulses and the mass loss was determined by weighing.

Besides air as the ambient gas, a control value was determined in a nitrogen atmosphere at environmental pressure. For a better comparison in all diagrams to follow the equivalent data for the GL are shown as well. The data for the GL are those with a Delrin pin of 15 mm length and 8 mm in diameter, if not specified otherwise.

31
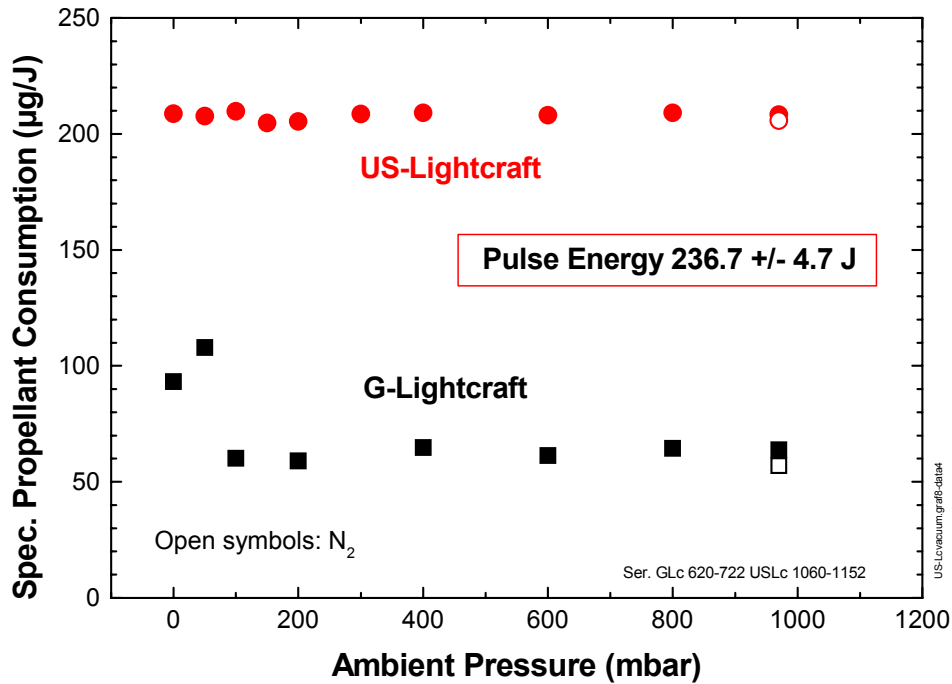
Fig. 26 - Specific propellant consumption vs. ambient pressure

Analogously to the findings for the GL the specific propellant consumption for the USL is independent of the pressure (Fig. 26). The value is 208 ± 2 µg/J. A chemical reaction with air on the Delrin surface can be excluded. This is also supported by the comparable value in the nitrogen atmosphere. However, the mass loss is more than 3 times higher than for the GL at the tested pulse energy level. This is attributed to the lower intensity on the long focal line, allowing the evaporation of more Delrin before the surface is shielded from the laser light. Because the pulse energy was equal for all data, the absolute mass loss has the same behavior. It can be re-calculated by multiplication with the pulse energy of 236.7 J. Note, that in contrast to the GL at pressures ≤ 50 mbar no increase in the vaporized Delrin mass has been observed.

Fig. 27 - Used Delrin rings. The lowest ring is unused .

An inspection of the used Delrin rings showed that the material is ablated not only along the focal line but over a considerable fraction of the exposed surface. (Fig. 27). It is also not homogenously removed but unveils a series of parallel circumferential lines that can be felt easily as tiny grooves. Before use the surface was smooth.
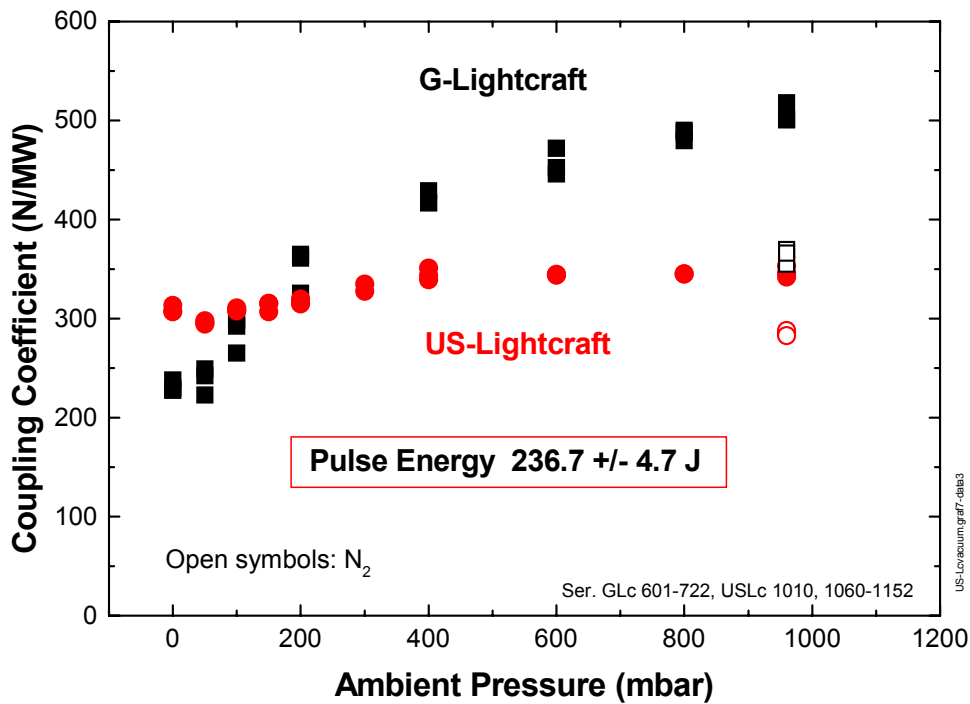
Fig. 28 - Coupling coefficient vs. ambient pressure

Quite in contrast to the GL the coupling coefficient c_m is also fairly independent of the ambient pressure (Fig. 28). There is a small increase in the pressure range below 400 mbar of 15 % from 300 N/MW to 345 N/MW. With this value about the same impulse is produced as with the GL in a nitrogen atmosphere of 1 bar. The nitrogen value for the USL at 1 bar is within experimental error comparable to the vacuum values.

As the control value in nitrogen suggests, only a slight effect of the reaction enthalpy of the Delrin vapor burning in air is found. Although movie pictures have shown a considerable cloud emanating from the lightcraft (see Fig. 8), most of the reaction apparently takes place outside of the range of the lightcraft and does not contribute to the thrust. In vacuum the coupling coefficient is higher than for the GL, probably a direct consequence of the higher evaporated mass.
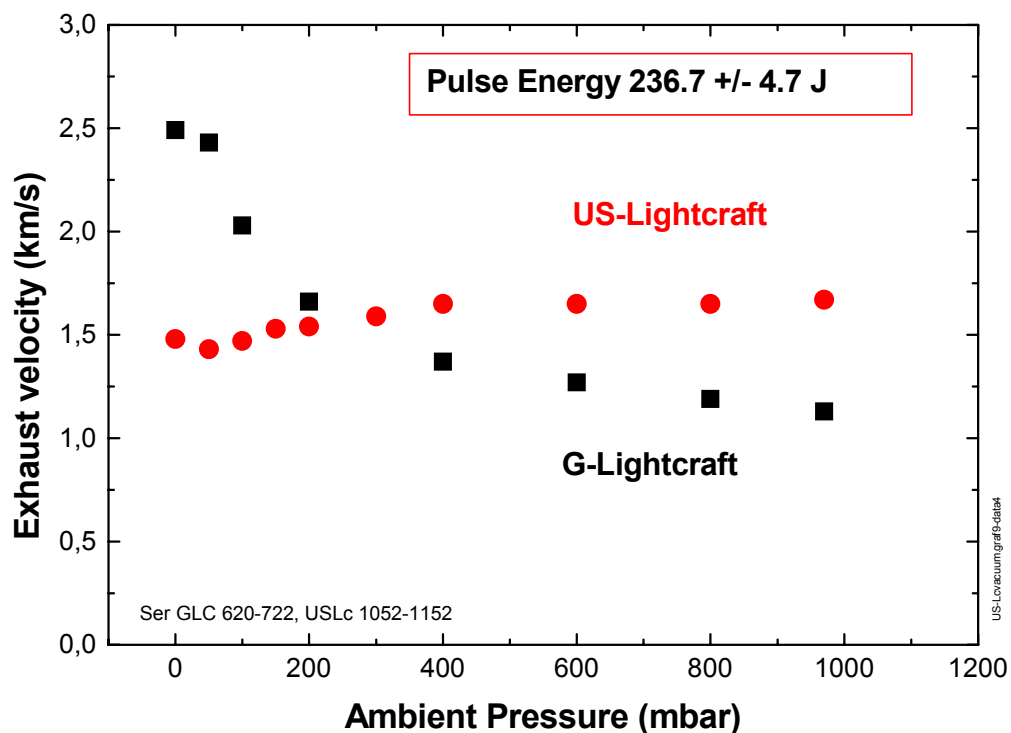
Fig. 29 - Average exhaust velocity vs. ambient pressure

The jet exhaust velocity can be exactly determined under vacuum conditions. A value of 1.5 km/s is derived (Fig. 29). As soon as residual air participates in the thrust process only approximate values can be determined, as shown in the evaluations for the GL. Because of the minor dependence of both, specific mass loss and coupling coefficient on pressure, the jet velocity also shows little dependence. Above 400 mbar it is virtually constant within experimental error and surpasses the value for the GL at atmospheric pressure. The jet efficiency in vacuum is $\eta_j = 21.4$ %.
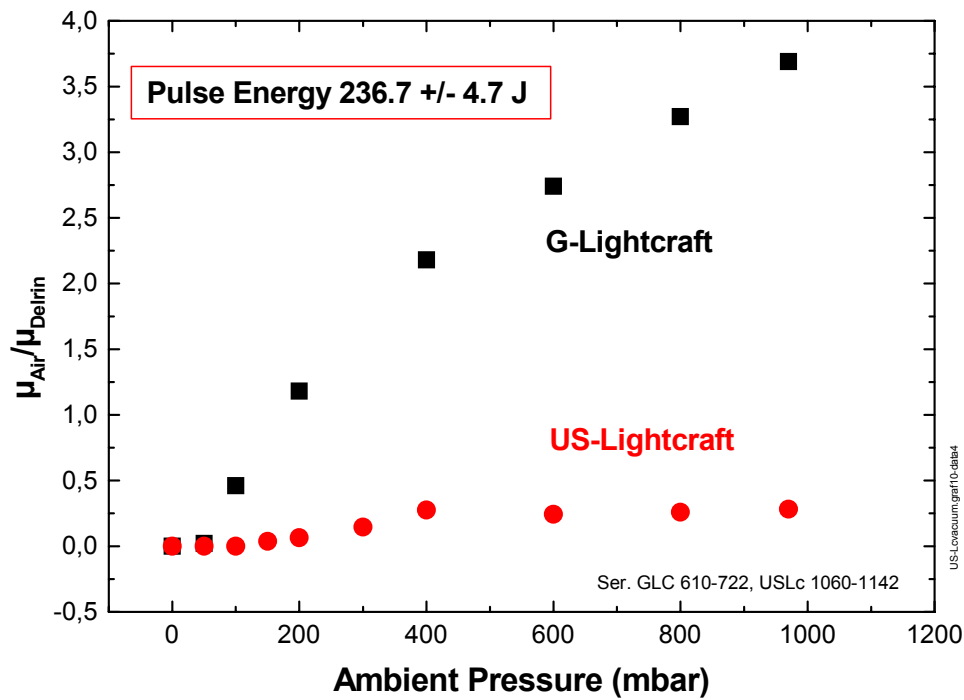
Fig. 30 - Mass ratio of exhausted gases vs. ambient pressure

The amount of participating air in the thrust mechanism is apparently small and does not exceed 25 % of the Delrin vapor mass (Fig. 30). This is very different from the GL. One reason for this discrepancy may be found in the radically different structure of the two lightcrafts. In the semi-closed bell shape a considerable amount of the enclosed air is accelerated and pushed out of the exit of the nozzle. In the open plug nozzle perhaps less volume is accelerated.

3.2.2 Dependency on the pulse energy in vacuum

In the experiments with the GL it has been found, that there is a marked difference whether the Delrin pin has a diameter of 8 or of 10 mm. The reason is probably the lower intensity on the surface and a wider illuminated area. This allows the evaporation over a broader area before the shielding effect sets in. Because this situation is closer to that encountered with the USL, both results for the GL have been enclosed in the following diagrams.

As Fig. 31 shows the absolute impulse for the USL is strictly linear and can be described as

$$I = 3.5 \cdot 10^{-4}\, E - 0.01\ (Ns)$$

35

There is a minimum energy of 30 J necessary to induce any impulse at all. Because of the linear nature of the impulse, the coupling coefficient must approach a finite value as $E \to \infty$. This value is 350 N/MW and cannot be surpassed.
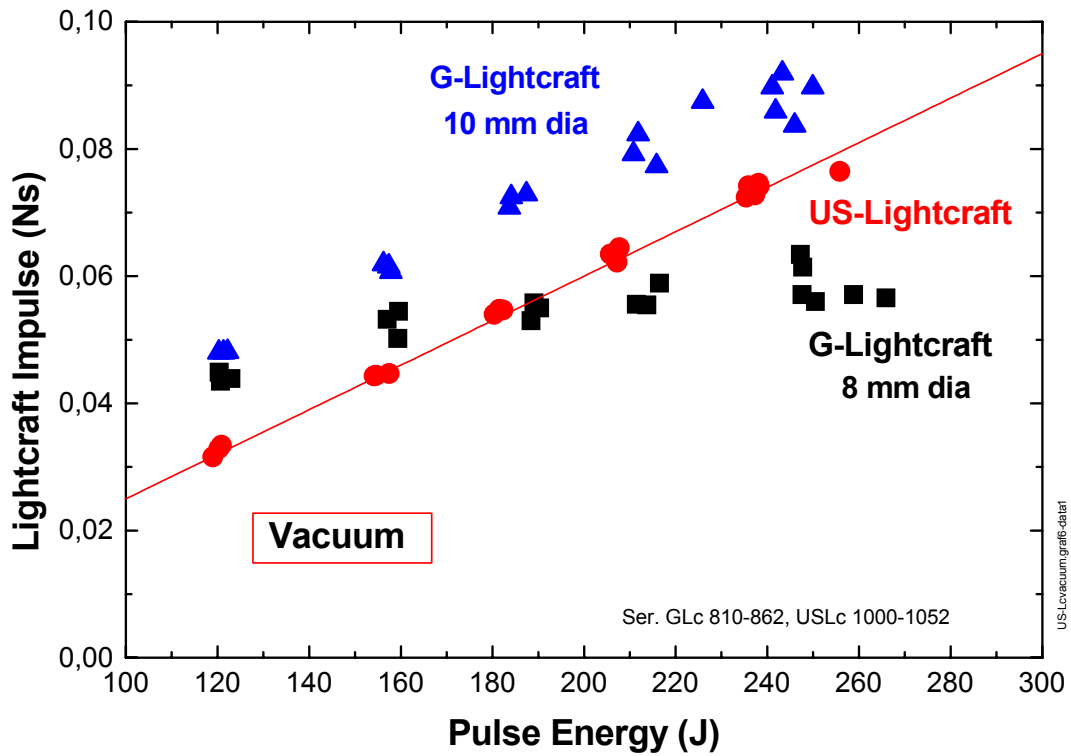
Fig. 31 - Lightcraft impulse in vacuum vs. laser pulse energy

Hence, the behavior of the two lightcrafts with respect to the coupling coefficient is very different (Fig. 32), if the 8 mm pin for the GL is considered: While for the USL the coupling coefficient starts for low energies with a relatively low value and then increases with the pulse energy (red dots), the GL shows the opposite behavior and for the 8 mm pin drops by almost a factor of two over the investigated energy range.

We believe, that the intensity in the focal region of the GL is already so high, that a substantial shielding effect occurs, that increases with the pulse energy. On the other hand, because of the much larger focal region in the USL the cut-off energy is not yet reached and only approached for the higher pulse energies. As the energy of the USL is increased to numbers, where the intensity on the Delrin surface reaches comparable

values as for the GL, then the same shielding effect is expected to set in and the coupling coefficient should then decrease again.
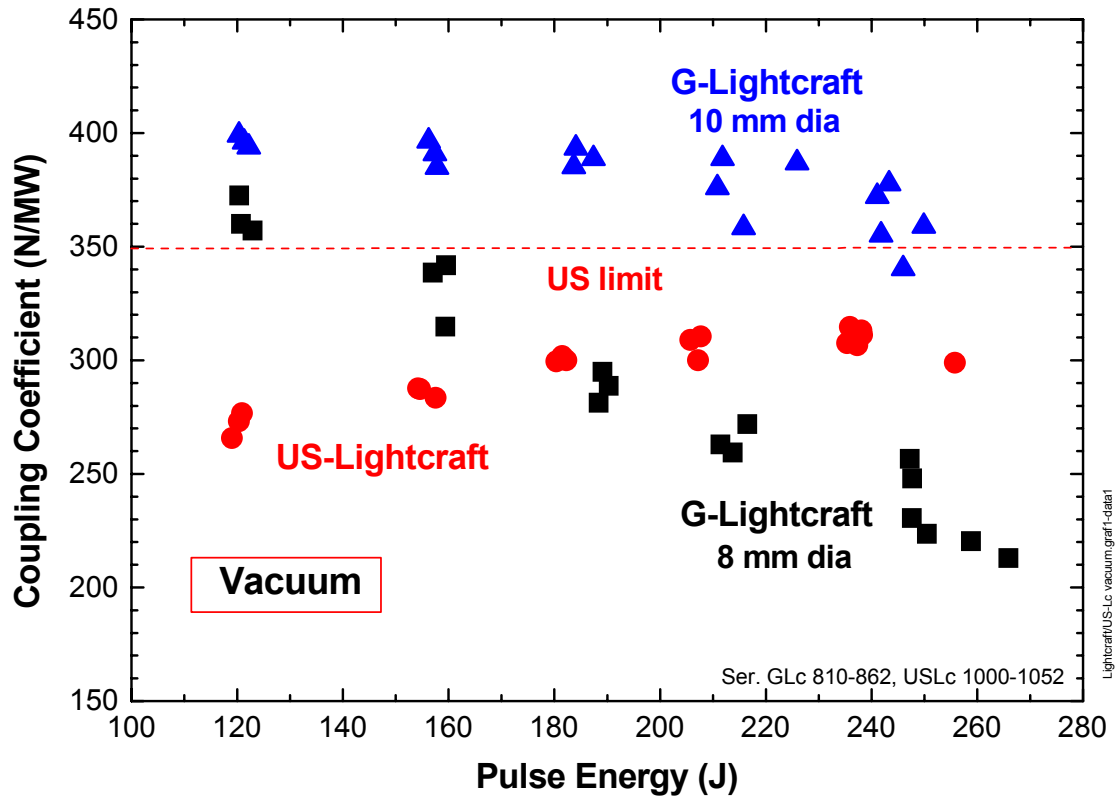
Fig. 32 – Coupling coefficient in vacuum vs. laser pulse energy

The assumption that the cut-off energy has not been reached yet for the USL is supported by the observed mass loss (Fig. 33). For the 8 mm pin the GL exhibits practically no change of the amount of produced Delrin vapor as the pulse energy is raised. So only a certain fixed fraction of the incoming laser light is actually dumped into the Delrin. In contrast, for the USL the mass loss increases proportionally to the pulse energy. Thus all the incident energy seems to be transfered into vapor. The functional dependence can be described as

$$m = (0.213 \, E - 0.33) \cdot 10^{-6} \quad (kg)$$
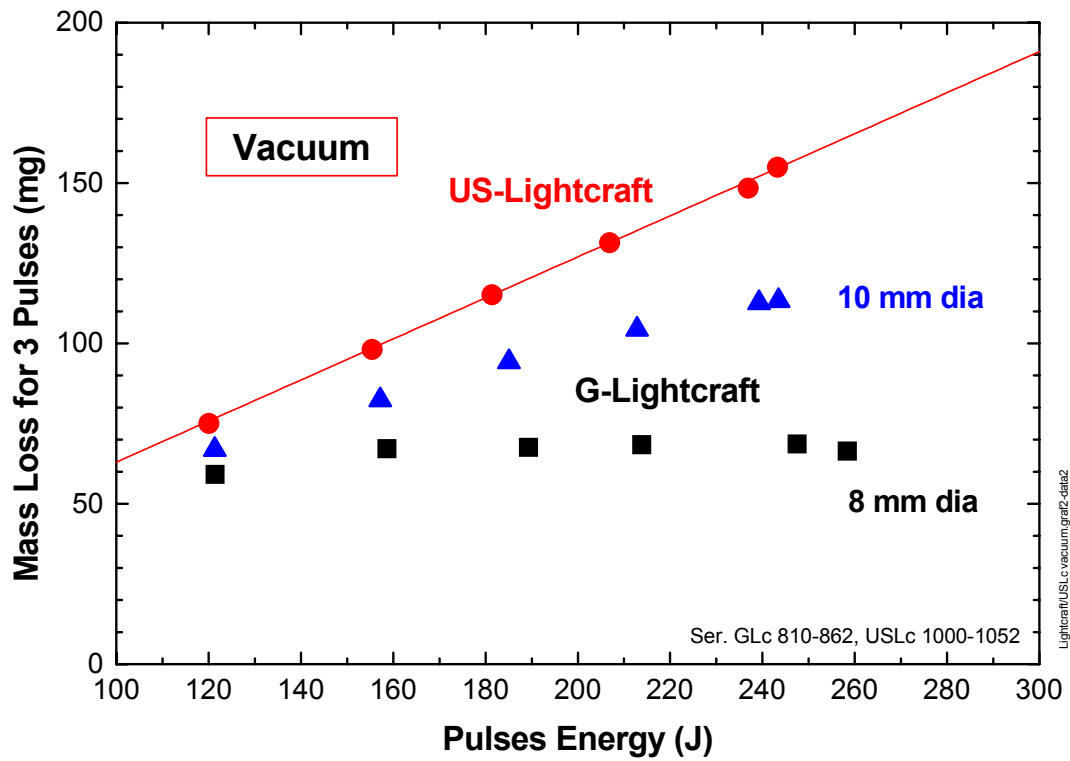
Fig. 33 - Mass loss for 3 pulses in vacuum vs. laser pulse energy
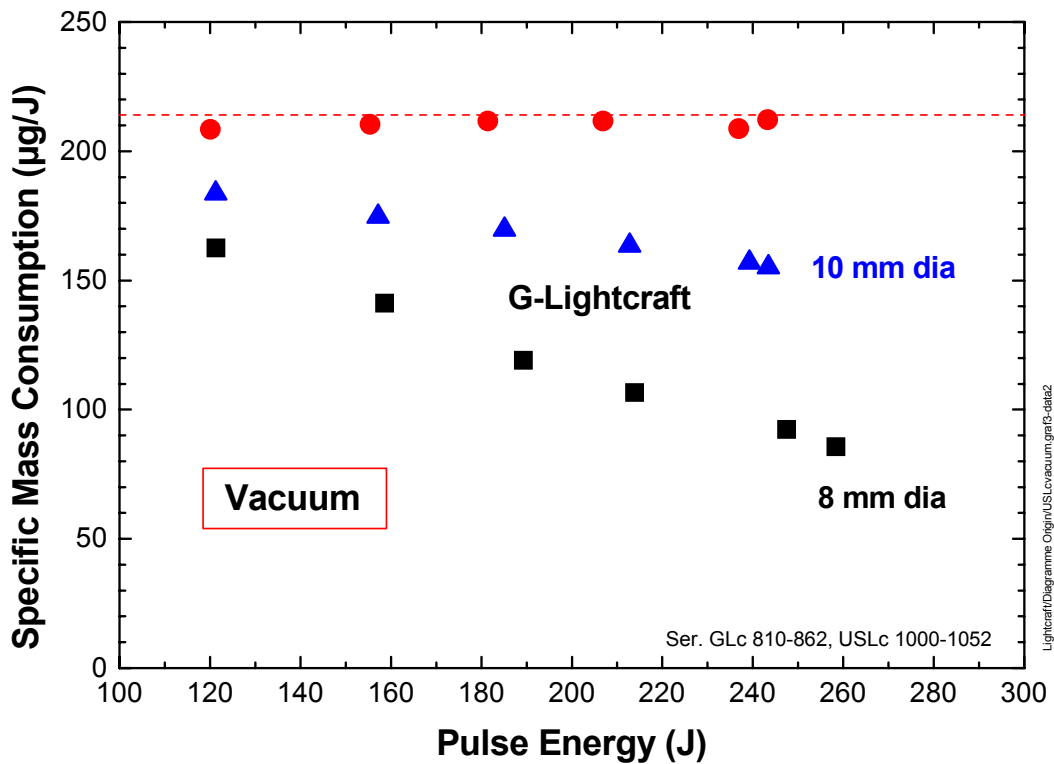
Fig. 34 - Specific propellant consumption in vacuum vs. laser pulse energy

can be directly written as a function of the mass loss

$$I = 1.64 \cdot 10^3 \, m - 9.46 \cdot 10^{-3}$$

In this and all the following diagrams the pulse energy is always the mean value of all 3 energies that acted on the Delrin ring before it was taken of, weighed and replaced by a new one for the next pulse energy level.

Because the mass loss is proportional to the pulse energy for the USL, the specific mass loss, μ, must be nearly independent and it must decrease for the GL. This is actually so, as seen in Fig. 34. The limiting value for $\mu = 213 \, \mu g/J$.

A low mass loss supports a high exhaust velocity, because of $v_{ex} = c_m / \mu$. Therefore, the exhaust velocity is higher for the GL (Fig. 35). The analytical function for the USL is also plotted in the diagram. The exhaust velocity barely reaches 1.5 km/s.

Because of this low exhaust velocity the jet efficiency for the USL is low, too (Fig. 36).
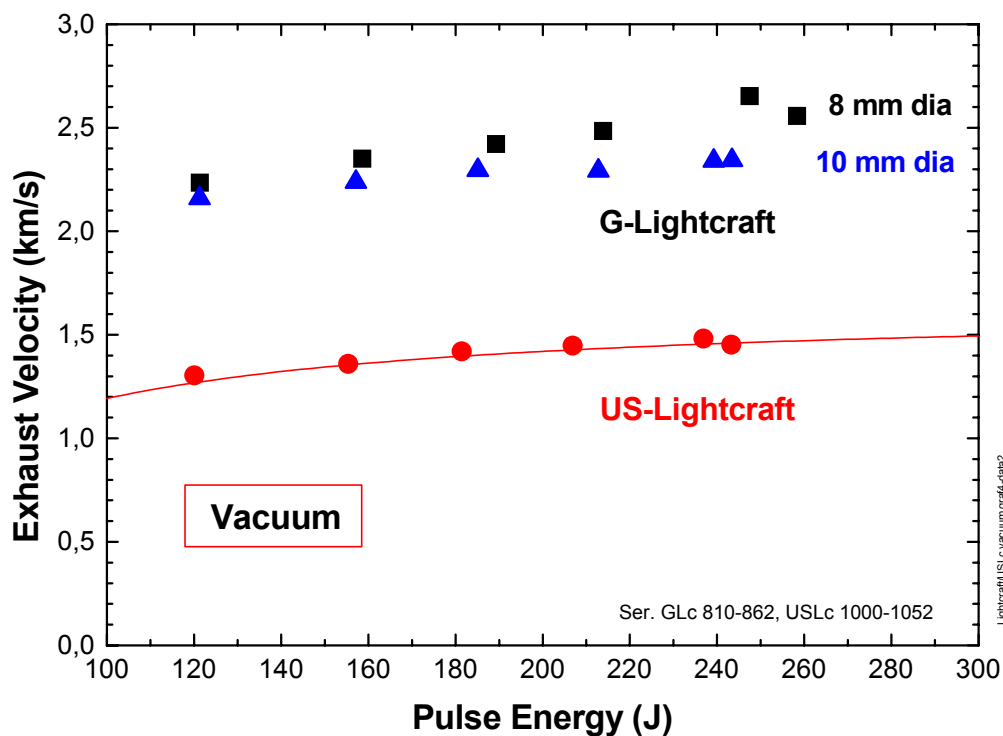
Fig. 35 - Average exhaust velocity in vacuum vs. laser pulse energy
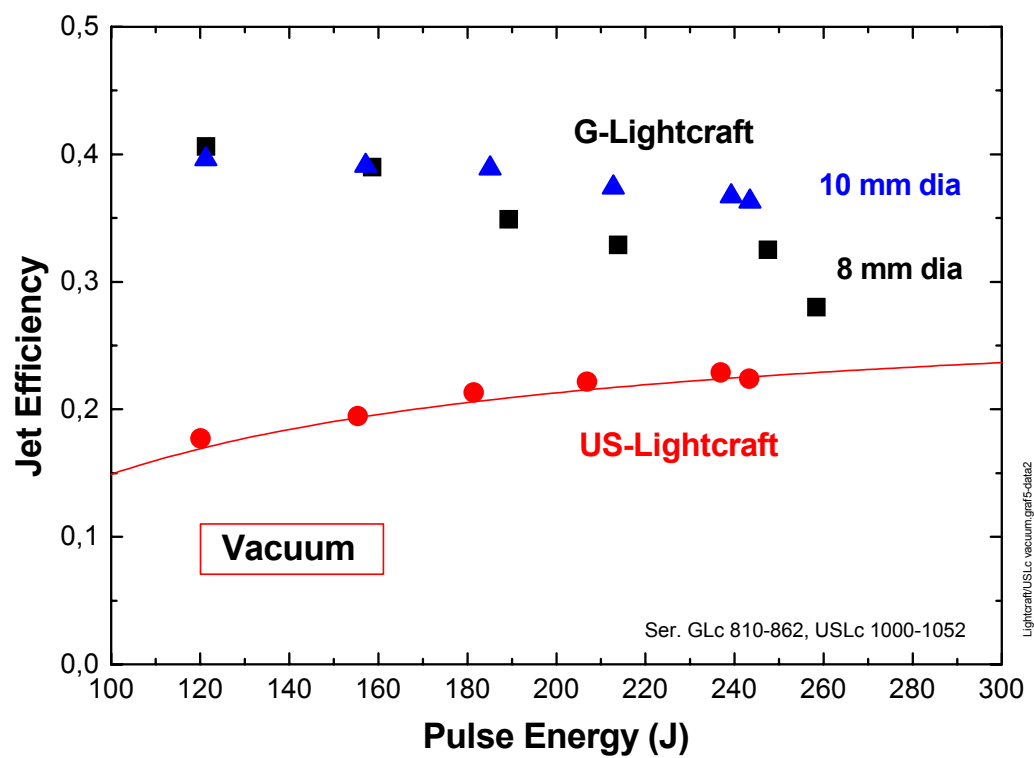
Fig. 36 - Jet efficiency in vacuum vs. laser pulse energy

4. DISCUSSION OF THE RESULTS

Several experimental results can serve as a basis for extrapolations and have consequences with respect to future investigations. The measurements described in this report are the only one at reduced environmental pressures and at vacuum in the recent past since the pioneering work in the USA of Pirri and Weiss in 1972[4] and in Russia by Ageev in 1980[5] .

1) The result of the measurements with the GL in air without additional propellant (Fig. 4) has an important consequence for the launching of lightcrafts. If the pressure is translated into values of altitude corresponding to the variation of the pressure in the normal atmosphere, the surprising result of Fig. 37 becomes apparent (in this diagram the curve for 128 J has been plotted): For an airbreathing propulsion the c_m-value and thus the thrust remains constant to an altitude of 11.2 km, before it begins to decrease. But at 20 km still half of the thrust is available. Finally, between 25 and 30 km it becomes so low that it can just about compensate the weight force and the acceleration goes to zero. It is thus possible to lift a lightcraft without using on-board propellant to an altitude where the air density is reduced considerably. The air density is responsible for the drag force and would require additional propellant. At the maximum altitude the propulsion must switch over to the rocket mode, utilizing propellant carried on board. Also a moderate acceleration can be applied now, as the lightcraft gains altitude and the drag force is further reduced. This launch procedure with a pure air breathing mode is impossible with the shape of the USL because no reproducible breakdown of air with sufficient impulse can be achieved, especially at lower pulse powers.

2) At very low pressures ($\leq$ 100 mbar) the use of an additional on-board propellant is indispensable. With an appropriate laser pulse that allows to dump the pulse energy fully into the propellant, i.e. a matched intensity at the surface of a solid propellant, a coupling coefficient of 400 N/MW for Delrin could be achieved in vacuum with the GL. The USL showed a definite upper limit at the slightly lower value of 350 N/MW.

3) Since the coupling coefficient with Delrin propellant in the GL decreases with increasing fluence (J/cm^2) at the target a threshold fluence must exist that is not yet reached for the USL with its much larger focal area. The physical mechanism that limits

41
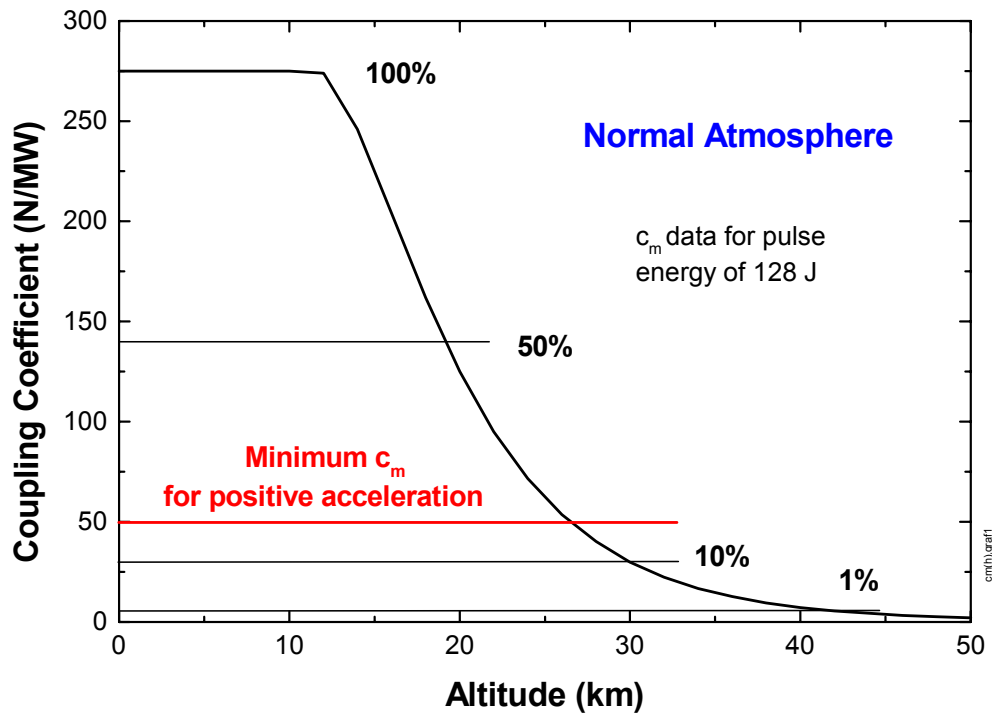
Fig. 37 - Coupling coefficient vs. flight altitude

the deposition of energy into the propellant is most likely the creation of LSD-waves (Laser Supported Detonation waves). LSD-waves absorb a certain fraction of the pulse energy at a location where it cannot contribute to the thrust. It has been found that the created impulse is directly proportional to the evaporated Delrin mass. Therefore, the vapor itself must be transparent to the laser radiation. Both properties, the cut-off of the laser beam after a certain time and the impossibility to deposit energy in the vapor call for a different laser radiation with respect to wavelength and pulse duration and for a different propellant material. To resolve the problem of inappropriate energy deposition investigations using short time imaging techniques should be carried out.

4) If instead of air alone another propellant is used during the ascent in the denser air a considerable increase in impulse can be obtained. At a pressure of 1 bar the coupling coefficient (for low pulse energy) in the bell shaped GL is increased by a factor of 2.7 (Fig. 15). A significant fraction of this increase is most likely associated with the combustion of propellant vapor in air (Fig. 7). Since this combustion occurs inside the thrust chamber of the GL it can contribute to the impulse. This effect is much less pronounced in the USL with its open thruster structure (Fig. 28). In the USL less air can be accelerated together with the Delrin as the air pressure increases (Fig. 30). It needs to

42

be found out by mission calculations which propulsion mode is more efficient in the overall transportation balance. Too high an acceleration in the denser atmosphere is uneconomical because of the quadratic increase of the drag force with the velocity. Fig. 38 shows the velocity vs. the altitude where the drag force becomes equal or twice as high as the weight force. If for the rise through the atmosphere the air breathing mode is preferred, then a bell shaped nozzle must be utilized. In addition, propellants should be investigated for their efficiency that release additional energy for instance by decomposition[6] or by a combustion process with air for a hybrid propulsion mode. The combustion of Delrin vapor with air delivered an additional propulsive effect down to a pressure of 400 mbar, corresponding to an altitude of 7 km in the normal atmosphere.

5) Due to the combustion effect the exact exhaust conditions could not be determined, except for full vacuum. Some means to determine the fraction of air in the exhaust gas should be developed. Independent of this deficiency it is clear that the obtained exhaust
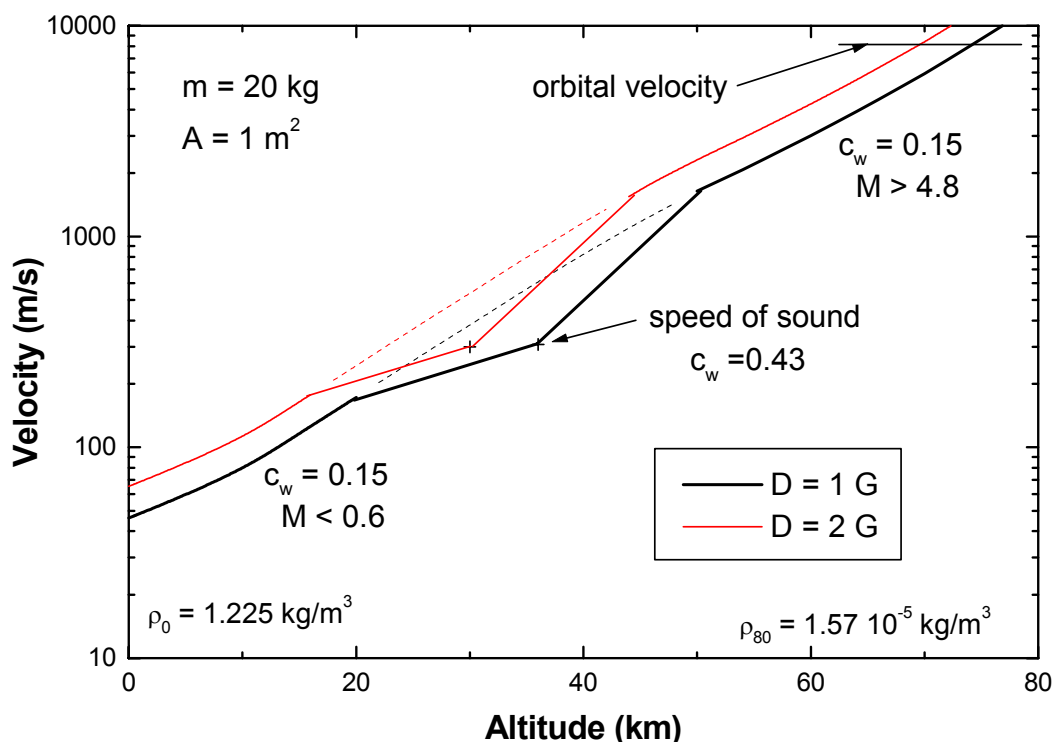
Fig. 38 - Example calculation for the flight velocity vs. altitude where the drag force assumes the same or the double value of the weight. The dip is due to an increase of the drag coefficient in the vicinity of Mach 1.

velocity in vacuum with a maximum of 2.6 km/s for the GL and only 1.5 km/s for the USL is entirely insufficient for launching satellites (Fig. 35). For such a mission a minimum of 6 km/s should be obtained. Again, for this purpose a different propellant is required that needs a higher energy for ablation / evaporation and allows the deposition of additional energy in the gaseous state.

6) The jet efficiency is an important quantity that defines the size of the laser for a certain flight application. It should be as high as possible for an effective propulsion as well as for the reduction of heat losses to the thrust chamber. A maximum value of 40 % has been found for the GL (Fig. 36), while for the USL an efficiency in excess of 25 % would require very high pulse energies. On the other hand, higher gas temperatures in the thrust chamber will lead to a higher non-recoverable inner energy in the gas (excitation, ionization …) and to increased radiation and thus reduce the efficiency again. A loss of about 30 % of the pulse energy to the wall by convection and radiation leaves another 30 % for non-recoverable losses.

7) The specific propellant consumption for Delrin seems to be limited to 213 µg/J and is a property of the particular propellant (Fig. 34). Lower values are apparently due to other effects. The specific propellant consumption is obviously independent of the ambient pressure, except for an unresolved increase at pressure below 50 mbar in the GL (Fig. 26).

8) It should be reminded that a decreasing tendency of the c_m-value with pulse energy does not necessarily mean that a higher energy does no more produce a higher impulse. It actually depends on the rate of decrease of c_m. For a constant c_m the impulse still grows in proportion to the pulse energy.

5. CONCLUSIONS

The goal of this study was the determination of the propulsive properties of a lightcraft in vacuum. Two lightcrafts of similar size but very different geometry have been successfully tested for the first time at pressures below the atmospheric pressure. With a pendulum in a vacuum tank the impulse on the lightcrafts has been determined for a variety of conditions: The ambient gas, air or nitrogen, has been used as the only

propellant and it has been supplemented or substituted with Delrin as a solid propellant. Various geometries for the propellant irradiation with the laser light have been investigated as well and showed the necessity to tailor the laser pulse to the propellant or vice versa for maximum performance. In particular, test with shorter pulse durations should be attempted and other wavelengths with sufficient pulse energy would be of interest as well. It has been found that with a proper shape of the light concentrating thrust chamber a launch with propelled altitudes up to 25 km can be performed in an air breathing propulsion mode. The consequent monitoring of the Delrin loss throughout the test sequences with solid propellant allowed the derivation of the exhaust properties, and hence the specific impulse, and the jet efficiency at least for full vacuum conditions (p $\leq$ 1 mbar). For intermediate pressure conditions a certain range of the exhaust properties could be given. The derived exhaust velocities have not exceeded 2.6 km/s and therefore the specific impulse of 265 s falls short of the requirements for a satellite launch. Other propellants must be tested for better performance and it is adviced to look more deeply into the physical mechanisms that are associated with the breakdown process and the formation of thrust. The investigated propellant Delrin was ideal for the experiments, because it did not produce any depositions. In that respect other propellants may be less convenient. Hybrid propulsion with a chemical energy component may considerably enhance the performance in the operating regime for satellite launches. Only two shapes of a thruster have been tested in this study. Other geometries should be looked at in more detail, too. It has been noticed several times that a more slender geometry of the bell-shaped lightcrafts could still improve the coupling coefficient[3,5,7].

References

1. W.O. Schall, W.L. Bohn, H.-A. Eckel, W. Mayerhofer, W. Riede, S. Walther, E. Zeyfang, "*US German lightcraft impulse measurements*", EOARD Report under contract no. F61775-00-WE033, April 2001.

2. C.W. Larson, F.B. Mead Jr., W.M. Kalliomaa, "*Energy conversion in laser propulsion II*", paper AIAA 2002-0632, January 2002.

3. W.O. Schall, W.L. Bohn, H.-A. Eckel, W. Mayerhofer, W. Riede, E. Zeyfang, "*Lightcraft experiments in Germany*", High-Power Laser Ablation III, Proc. SPIE Vol.4065, pp. 472-481, 2000.

4. A.N. Pirri, R.F. Weiss, "*Laser propulsion*", paper AIAA 72-719, June 1972.

5. V.P. Ageev, A.I. Barchukov, F.V. Bunkin, V.I. Konov, V.P. Korobeinikov, B.V. Butjatin, V.M. Hudjakov, "*Experimental and theoretical modeling of laser propulsion*", Acta Astronautica, Vol. 7, pp. 79-90, 1980.

6. R.A. Liukonen, " *Laser jet propulsion*", Proc. SPIE Vol. 3574, pp. 470-474, 1998

7. L.N. Myrabo, M.A. Libeau, E.D. Meloney, R.L. Bracken, "*Pulsed Laser propulsion performance of 11-cm parabolic "Bell" engines within the atmosphere*", paper AIAA 2002-2206, May 2002.

Appendix

Tables of measurements and evaluation.

Table A – German Lightcraft

Stable resonator

Total pendulum mass: 438.3 g

Pendulum length (center of mass): 645 mm

#	Comment	Press. (mbar)	Energy (V)	Displace-ment (mm)	Laser Energy (J)	Angle (°)	Height (mm)	Energy (J)	Velocity (m/s)	Impulse (N*s)	Coupling (N/MW)	Mass loss (mg)
20	no vessel	960	0.0779	42.2	238.2	3.750	1.381	0.005939	1.65E-01	7.22E-02	302.94	
21	no vessel	960	0.0788	42.8	240.5	3.805	1.422	0.006114	1.67E-01	7.32E-02	304.45	
30	no vessel	960	0.0947	43.5	284.8	3.867	1.468	0.006313	1.70E-01	7.44E-02	261.18	
31	no vessel	960	0.0946	43.7	284.7	3.884	1.481	0.006368	1.70E-01	7.47E-02	262.47	
32	no vessel	960	0.0935	43.1	281.6	3.830	1.441	0.006195	1.68E-01	7.37E-02	261.67	
33	no vessel	960	0.1041	47.9	310.4	4.260	1.782	0.007660	1.87E-01	8.19E-02	263.98	
34	no vessel	960	0.1045	48.3	311.5	4.293	1.810	0.007782	1.88E-01	8.26E-02	265.16	
35	no vessel	960	0.1047	47.6	312.0	4.231	1.758	0.007558	1.86E-01	8.14E-02	260.87	
36	no vessel	960	0.0785	35.9	239.8	3.186	0.997	0.004286	1.40E-01	6.13E-02	255.60	
37	no vessel	960	0.0788	36.2	240.6	3.212	1.013	0.004356	1.41E-01	6.18E-02	256.79	
38	no vessel	960	0.0782	35.8	239.0	3.183	0.995	0.004279	1.40E-01	6.12E-02	256.23	
39	no vessel	960	0.0673	30.5	207.6	2.711	0.722	0.003105	1.19E-01	5.22E-02	251.30	
40	no vessel	960	0.0677	30.8	208.7	2.738	0.736	0.003166	1.20E-01	5.27E-02	252.40	
41	no vessel	960	0.0675	31.0	208.4	2.753	0.744	0.003201	1.21E-01	5.30E-02	254.22	
42	no vessel	960	0.0553	25.2	172.5	2.241	0.493	0.002122	9.84E-02	4.31E-02	250.06	
43	no vessel	960	0.0555	25.3	173.1	2.249	0.497	0.002137	9.87E-02	4.33E-02	250.01	
44	no vessel	960	0.0556	25.3	173.5	2.243	0.494	0.002125	9.85E-02	4.32E-02	248.80	
45	no vessel	960	0.0417	17.6	131.7	1.565	0.241	0.001035	6.87E-02	3.01E-02	228.64	
46	no vessel	960	0.0415	17.8	131.1	1.578	0.245	0.001051	6.93E-02	3.04E-02	231.53	
47	no vessel	960	0.0418	17.8	131.8	1.581	0.246	0.001056	6.94E-02	3.04E-02	230.76	
50		960	0.0420	16.5	132.7	1.463	0.210	0.000904	6.42E-02	2.82E-02	212.15	
51		960	0.0392	15.9	124.0	1.412	0.196	0.000843	6.20E-02	2.72E-02	219.20	
52		960	0.0394	16.6	124.8	1.474	0.213	0.000917	6.47E-02	2.84E-02	227.26	
53		960	0.0397	17.2	125.5	1.530	0.230	0.000988	6.72E-02	2.94E-02	234.63	

#	Comment	Press. (mbar)	Energy (V)	Displacement (mm)	Laser Energy (J)	Angle (°)	Height (mm)	Energy (J)	Velocity (m/s)	Impulse (N*s)	Coupling (N/MW)	Mass loss (mg)
54		960	0.0650	31.1	201.1	2.760	0.748	0.003218	1.21E-01	5.31E-02	264.09	
55		960	0.0641	30.0	198.2	2.666	0.698	0.003002	1.17E-01	5.13E-02	258.76	
56		960	0.0645	30.4	199.6	2.698	0.715	0.003074	1.18E-01	5.19E-02	260.11	
57		960	0.0880	44.4	266.4	3.943	1.527	0.006565	1.73E-01	7.59E-02	284.75	
58		960	0.0890	43.0	269.0	3.824	1.436	0.006174	1.68E-01	7.36E-02	273.44	
59		960	0.0885	43.2	267.8	3.841	1.449	0.006229	1.69E-01	7.39E-02	275.93	
60	Air	0	0.0917	7.4	276.6	0.660	0.043	0.000184	2.90E-02	1.27E-02	45.91	
61	Air	0	0.0896	1.9	270.8	0.171	0.003	0.000012	7.50E-03	3.29E-03	12.13	
62	Air	0	0.0902	0.8	272.4	0.075	0.001	0.000002	3.31E-03	1.45E-03	5.33	
70	Air	200	0.0906	34.0	273.5	3.023	0.898	0.003860	1.33E-01	5.82E-02	212.68	
71	Air	200	0.0894	34.0	270.3	3.023	0.898	0.003860	1.33E-01	5.82E-02	215.18	
72	Air	200	0.0912	34.1	275.1	3.031	0.902	0.003880	1.33E-01	5.83E-02	211.98	
80	Air	400	0.0919	43.5	277.1	3.868	1.470	0.006319	1.70E-01	7.44E-02	268.56	
82	Air	400	0.0905	43.4	273.3	3.852	1.457	0.006264	1.69E-01	7.41E-02	271.09	
84	Air	400	0.0925	42.4	279.0	3.767	1.394	0.005992	1.65E-01	7.25E-02	259.80	
90	Air	600	0.0925	42.3	278.9	3.761	1.389	0.005972	1.65E-01	7.24E-02	259.47	
92	Air	600	0.0909	42.3	274.4	3.762	1.390	0.005975	1.65E-01	7.24E-02	263.71	
93	Air	600	0.0923	46.4	278.2	4.122	1.668	0.007173	1.81E-01	7.93E-02	285.06	
100	Air	800	0.0896	40.7	270.8	3.616	1.284	0.005521	1.59E-01	6.96E-02	256.94	
102	Air	800	0.0918	41.5	276.8	3.687	1.335	0.005740	1.62E-01	7.09E-02	256.28	
103	Air	800	0.0915	41.4	276.0	3.679	1.329	0.005716	1.61E-01	7.08E-02	256.49	
110	Air	50	0.0908	18.6	274.1	1.653	0.268	0.001154	7.26E-02	3.18E-02	116.07	
111	Air	50	0.0903	18.8	272.8	1.671	0.274	0.001179	7.34E-02	3.22E-02	117.87	
112	Air	50	0.0916	18.5	276.2	1.641	0.264	0.001137	7.20E-02	3.16E-02	114.29	

#	Comment	Press. (mbar)	Energy (V)	Displace-ment (mm)	Laser Energy (J)	Angle (°)	Height (mm)	Energy (J)	Velocity (m/s)	Impulse (N*s)	Coupling (N/MW)	Mass loss (mg)
120	Air	100	0.0913	25.6	275.5	2.270	0.506	0.002176	9.96E-02	4.37E-02	158.51	
121	Air	100	0.0918	25.6	277.0	2.276	0.509	0.002188	9.99E-02	4.38E-02	158.12	
122	Air	100	0.0915	26.0	276.1	2.312	0.525	0.002258	1.02E-01	4.45E-02	161.13	
130	Air	150	0.0919	31.3	277.3	2.783	0.761	0.003272	1.22E-01	5.36E-02	193.13	
131	Air	150	0.0916	31.2	276.5	2.769	0.753	0.003238	1.22E-01	5.33E-02	192.72	
132	Air	150	0.0905	31.0	273.2	2.751	0.744	0.003197	1.21E-01	5.29E-02	193.75	
140	Air	300	0.0915	39.1	276.1	3.474	1.185	0.005096	1.52E-01	6.68E-02	242.09	
141	Air	300	0.0911	40.3	274.9	3.582	1.260	0.005419	1.57E-01	6.89E-02	250.72	
142	Air	300	0.0908	38.8	274.2	3.451	1.169	0.005028	1.51E-01	6.64E-02	242.15	
150	Air	25	0.0892	12.3	269.8	1.090	0.117	0.000502	4.79E-02	2.10E-02	77.75	
151	Air	25	0.0904	12.5	273.0	1.107	0.120	0.000517	4.86E-02	2.13E-02	78.03	
152	Air	25	0.0904	12.2	273.1	1.086	0.116	0.000499	4.77E-02	2.09E-02	76.56	
160	Air	25	0.0669	10.2	206.4	0.903	0.080	0.000344	3.96E-02	1.74E-02	84.13	
161	Air	25	0.0656	9.8	202.8	0.870	0.074	0.000319	3.82E-02	1.67E-02	82.51	
162	Air	25	0.0646	9.4	199.8	0.832	0.068	0.000292	3.65E-02	1.60E-02	80.11	
170	Air	50	0.0658	14.6	203.3	1.299	0.166	0.000712	5.70E-02	2.50E-02	122.94	
171	Air	50	0.0657	14.1	203.1	1.254	0.155	0.000665	5.51E-02	2.41E-02	118.84	
172	Air	50	0.0652	14.3	201.7	1.270	0.159	0.000682	5.58E-02	2.44E-02	121.19	
180	Air	100	0.0665	20.1	205.2	1.782	0.312	0.001341	7.82E-02	3.43E-02	167.09	
181	Air	100	0.0655	20.6	202.4	1.832	0.330	0.001417	8.04E-02	3.52E-02	174.14	
182	Air	100	0.0650	20.0	201.1	1.774	0.309	0.001329	7.79E-02	3.41E-02	169.73	
191	Air	150	0.0653	24.1	201.9	2.144	0.451	0.001941	9.41E-02	4.12E-02	204.31	
192	Air	150	0.0653	24.0	201.9	2.130	0.446	0.001917	9.35E-02	4.10E-02	203.04	
193	Air	150	0.0662	24.5	204.5	2.172	0.463	0.001993	9.54E-02	4.18E-02	204.41	

#	Comment	Press. (mbar)	Energy (V)	Displace-ment (mm)	Laser Energy (J)	Angle (°)	Height (mm)	Energy (J)	Velocity (m/s)	Impulse (N*s)	Coupling (N/MW)	Mass loss (mg)
200	Air	200	0.0661	26.6	204.1	2.360	0.547	0.002353	1.04E-01	4.54E-02	222.48	
201	Air	200	0.0653	26.4	201.8	2.344	0.539	0.002320	1.03E-01	4.51E-02	223.49	
202	Air	200	0.0652	26.8	201.6	2.377	0.555	0.002387	1.04E-01	4.57E-02	226.84	
210	Air	300	0.0659	29.4	203.7	2.613	0.671	0.002883	1.15E-01	5.03E-02	246.82	
211	Air	300	0.0655	30.8	202.5	2.739	0.737	0.003168	1.20E-01	5.27E-02	260.22	
212	Air	300	0.0659	29.2	203.7	2.592	0.660	0.002838	1.14E-01	4.99E-02	244.89	
220	Air	400	0.0659	31.2	203.5	2.769	0.753	0.003238	1.22E-01	5.33E-02	261.81	
221	Air	400	0.0655	30.4	202.5	2.702	0.717	0.003084	1.19E-01	5.20E-02	256.83	
222	Air	400	0.0651	29.8	201.2	2.651	0.690	0.002968	1.16E-01	5.10E-02	253.46	
230	Air	600	0.0658	30.3	203.3	2.694	0.713	0.003064	1.18E-01	5.18E-02	254.96	
231	Air	600	0.0654	29.9	202.2	2.659	0.694	0.002986	1.17E-01	5.12E-02	252.99	
232	Air	600	0.0653	30.0	201.8	2.667	0.699	0.003004	1.17E-01	5.13E-02	254.33	
240	Air	800	0.0665	29.7	205.3	2.642	0.686	0.002948	1.16E-01	5.08E-02	247.58	
241	Air	800	0.0658	30.7	203.2	2.723	0.728	0.003131	1.20E-01	5.24E-02	257.81	
242	Air	800	0.0661	30.8	204.3	2.737	0.736	0.003164	1.20E-01	5.27E-02	257.80	
250	Air	960	0.0668	30.5	206.2	2.708	0.720	0.003097	1.19E-01	5.21E-02	252.67	
251	Air	960	0.0657	29.4	203.2	2.608	0.668	0.002873	1.15E-01	5.02E-02	247.03	
252	Air	960	0.0656	30.1	202.6	2.672	0.701	0.003016	1.17E-01	5.14E-02	253.74	
260	Air	25	0.0408	6.3	129.1	0.557	0.031	0.000131	2.45E-02	1.07E-02	83.10	
261	Air	25	0.0408	5.6	129.0	0.497	0.024	0.000105	2.18E-02	9.57E-03	74.23	
262	Air	25	0.0406	5.8	128.3	0.513	0.026	0.000111	2.25E-02	9.88E-03	76.96	
270	Air	50	0.0412	9.9	130.0	0.876	0.075	0.000324	3.84E-02	1.69E-02	129.60	
271	Air	50	0.0397	9.6	125.7	0.851	0.071	0.000306	3.74E-02	1.64E-02	130.30	
272	Air	50	0.0404	9.7	127.7	0.859	0.073	0.000312	3.77E-02	1.65E-02	129.44	

#	Comment	Press. (mbar)	Energy (V)	Displace-ment (mm)	Laser Energy (J)	Angle (°)	Height (mm)	Energy (J)	Velocity (m/s)	Impulse (N*s)	Coupling (N/MW)	Mass loss (mg)
280	Air	100	0.0412	13.9	130.3	1.238	0.151	0.000648	5.44E-02	2.38E-02	182.92	
281	Air	100	0.0406	14.1	128.3	1.253	0.154	0.000663	5.50E-02	2.41E-02	187.87	
282	Air	100	0.0406	13.8	128.3	1.229	0.148	0.000638	5.40E-02	2.37E-02	184.32	
290	Air	150	0.0408	17.0	128.9	1.512	0.225	0.000966	6.64E-02	2.91E-02	225.71	
291	Air	150	0.0413	16.8	130.4	1.492	0.219	0.000941	6.55E-02	2.87E-02	220.14	
292	Air	150	0.0412	17.3	130.0	1.532	0.231	0.000992	6.73E-02	2.95E-02	226.77	
300	Air	200	0.0427	18.6	134.6	1.648	0.267	0.001147	7.23E-02	3.17E-02	235.55	
301	Air	200	0.0406	18.9	128.2	1.677	0.276	0.001188	7.36E-02	3.23E-02	251.68	
302	Air	200	0.0410	18.8	129.6	1.672	0.275	0.001181	7.34E-02	3.22E-02	248.17	
310	Air	300	0.0404	18.2	127.9	1.614	0.256	0.001100	7.09E-02	3.11E-02	242.91	
312	Air	300	0.0402	18.9	127.3	1.680	0.277	0.001192	7.37E-02	3.23E-02	254.01	
313	Air	300	0.0406	18.8	128.3	1.672	0.275	0.001181	7.34E-02	3.22E-02	250.76	
320	Air	400	0.0412	18.5	130.1	1.643	0.265	0.001141	7.21E-02	3.16E-02	242.98	
321	Air	400	0.0404	18.3	127.7	1.621	0.258	0.001110	7.12E-02	3.12E-02	244.21	
322	Air	400	0.0410	18.0	129.6	1.601	0.252	0.001082	7.03E-02	3.08E-02	237.62	
330	Air	600	0.0414	18.7	130.7	1.659	0.270	0.001162	7.28E-02	3.19E-02	244.18	
331	Air	600	0.0413	18.5	130.4	1.640	0.264	0.001136	7.20E-02	3.16E-02	242.00	
332	Air	600	0.0409	18.9	129.3	1.675	0.276	0.001186	7.36E-02	3.22E-02	249.28	
340	Air	800	0.0411	19.5	130.0	1.736	0.296	0.001273	7.62E-02	3.34E-02	257.00	
341	Air	800	0.0404	18.6	127.8	1.651	0.268	0.001151	7.25E-02	3.18E-02	248.51	
342	Air	800	0.0411	19.1	130.0	1.695	0.282	0.001213	7.44E-02	3.26E-02	250.95	
350	Air	960	0.0416	16.4	131.2	1.460	0.209	0.000900	6.41E-02	2.81E-02	213.99	
351	Air	960	0.0415	16.7	131.1	1.479	0.215	0.000924	6.49E-02	2.85E-02	217.06	
352	Air	960	0.0413	16.3	130.6	1.449	0.206	0.000887	6.36E-02	2.79E-02	213.52	

#	Comment	Press. (mbar)	Energy (V)	Displace-ment (mm)	Laser Energy (J)	Angle (°)	Height (mm)	Energy (J)	Velocity (m/s)	Impulse (N*s)	Coupling (N/MW)	Mass loss (mg)
360	Air	25	0.0982	12.7	294.5	1.127	0.125	0.000537	4.95E-02	2.17E-02	73.66	
361	Air	25	0.0997	12.9	298.6	1.141	0.128	0.000550	5.01E-02	2.20E-02	73.56	
362	Air	25	0.0995	12.6	297.9	1.117	0.122	0.000527	4.90E-02	2.15E-02	72.14	
370	Air	50	0.0964	18.6	289.5	1.654	0.269	0.001156	7.26E-02	3.18E-02	109.93	
371	Air	50	0.0984	18.9	295.0	1.677	0.276	0.001188	7.36E-02	3.23E-02	109.40	
372	Air	50	0.0994	18.9	297.7	1.676	0.276	0.001187	7.36E-02	3.23E-02	108.33	
380	Air	100	0.1009	26.4	301.8	2.343	0.539	0.002318	1.03E-01	4.51E-02	149.36	
381	Air	100	0.1002	26.4	299.9	2.348	0.542	0.002328	1.03E-01	4.52E-02	150.65	
382	Air	100	0.0937	25.6	282.1	2.272	0.507	0.002179	9.97E-02	4.37E-02	154.95	
390	Air	150	0.1003	31.1	300.2	2.760	0.748	0.003218	1.21E-01	5.31E-02	176.93	
391	Air	150	0.0990	30.8	296.7	2.740	0.737	0.003170	1.20E-01	5.27E-02	177.66	
392	Air	150	0.0958	30.8	287.8	2.737	0.736	0.003164	1.20E-01	5.27E-02	182.99	
400	Air	200	0.1002	34.7	299.9	3.079	0.931	0.004004	1.35E-01	5.92E-02	197.56	
401	Air	200	0.0961	34.8	288.7	3.088	0.937	0.004027	1.36E-01	5.94E-02	205.82	
402	Air	200	0.0991	34.9	296.8	3.099	0.943	0.004055	1.36E-01	5.96E-02	200.86	
410	Air	300	0.0995	40.0	297.9	3.554	1.240	0.005333	1.56E-01	6.84E-02	229.55	
411	Air	300	0.0993	40.2	297.4	3.570	1.251	0.005381	1.57E-01	6.87E-02	230.96	
412	Air	300	0.0988	40.0	296.1	3.556	1.242	0.005341	1.56E-01	6.84E-02	231.11	
420	Air	400	0.1006	43.3	301.0	3.849	1.455	0.006255	1.69E-01	7.40E-02	246.03	
421	Air	400	0.0966	42.9	290.0	3.812	1.427	0.006137	1.67E-01	7.33E-02	252.91	
422	Air	400	0.1007	43.6	301.2	3.873	1.473	0.006333	1.70E-01	7.45E-02	247.34	
430	Air	500	0.0928	45.3	279.6	4.026	1.591	0.006843	1.77E-01	7.74E-02	277.03	
431	Air	500	0.0960	43.5	288.5	3.864	1.466	0.006304	1.70E-01	7.43E-02	257.71	
432	Air	500	0.1001	48.5	299.6	4.308	1.823	0.007837	1.89E-01	8.29E-02	276.63	

#	Comment	Press. (mbar)	Energy (V)	Displacement (mm)	Laser Energy (J)	Angle (°)	Height (mm)	Energy (J)	Velocity (m/s)	Impulse (N*s)	Coupling (N/MW)	Mass loss (mg)
440	Air	600	0.1015	47.4	303.4	4.209	1.739	0.007479	1.85E-01	8.10E-02	266.87	
444	Air	600	0.0950	43.9	285.7	3.902	1.495	0.006429	1.71E-01	7.51E-02	262.75	
447	Air	600	0.0937	46.5	282.2	4.131	1.675	0.007204	1.81E-01	7.95E-02	281.56	
452	Air	800	0.0864	41.3	262.0	3.669	1.322	0.005685	1.61E-01	7.06E-02	269.41	
453	Air	800	0.0956	43.0	287.3	3.823	1.435	0.006172	1.68E-01	7.36E-02	256.05	
454	Air	800	0.0985	44.4	295.3	3.942	1.526	0.006562	1.73E-01	7.58E-02	256.81	
455	Air	800	0.0904	40.4	273.0	3.590	1.266	0.005443	1.58E-01	6.91E-02	253.01	
460	Air	960	0.0913	42.1	275.5	3.743	1.376	0.005916	1.64E-01	7.20E-02	261.42	
461	Air	960	0.0977	42.5	293.2	3.773	1.398	0.006012	1.66E-01	7.26E-02	247.59	
462	Air	960	0.0934	42.0	281.4	3.729	1.365	0.005871	1.64E-01	7.17E-02	254.95	
463	Air	960	0.0914	41.0	275.8	3.642	1.302	0.005600	1.60E-01	7.01E-02	254.05	
501	Delrin	0	0.0907	30.7	273.9	2.724	0.729	0.003133	1.20E-01	5.24E-02	191.31	
502	Delrin	0	0.0923	31.5	278.4	2.795	0.767	0.003299	1.23E-01	5.38E-02	193.17	
503	Delrin	0	0.0909	29.7	274.4	2.642	0.686	0.002948	1.16E-01	5.08E-02	185.27	
504	Delrin	0	0.0908	29.6	274.2	2.631	0.680	0.002922	1.15E-01	5.06E-02	184.57	
505	Delrin	0	0.0914	28.2	275.7	2.503	0.615	0.002645	1.10E-01	4.82E-02	174.63	102.3
601	Delrin	0	0.0849	34.3	257.8	3.047	0.912	0.003921	1.34E-01	5.86E-02	227.40	
602	Delrin	0	0.0800	34.0	244.0	3.018	0.895	0.003846	1.32E-01	5.81E-02	237.98	
603	Delrin	0	0.0792	32.5	241.6	2.887	0.819	0.003521	1.27E-01	5.56E-02	229.94	69.3
610	Delrin	50	0.0800	34.6	243.9	3.072	0.927	0.003986	1.35E-01	5.91E-02	242.36	
612	Delrin	50	0.0802	35.6	244.6	3.165	0.984	0.004231	1.39E-01	6.09E-02	249.03	
614	Delrin	50	0.0799	31.8	243.6	2.822	0.782	0.003364	1.24E-01	5.43E-02	222.95	79
620	Delrin	100	0.0787	37.3	240.4	3.314	1.079	0.004637	1.45E-01	6.38E-02	265.27	
621	Delrin	100	0.0810	43.1	246.8	3.828	1.439	0.006186	1.68E-01	7.36E-02	298.41	

#	Comment	Press. (mbar)	Energy (V)	Displace-ment (mm)	Laser Energy (J)	Angle (°)	Height (mm)	Energy (J)	Velocity (m/s)	Impulse (N*s)	Coupling (N/MW)	Mass loss (mg)
622	Delrin	100	0.0801	41.8	244.3	3.713	1.354	0.005821	1.63E-01	7.14E-02	292.42	44
630	Delrin	200	0.0792	46.1	241.7	4.092	1.644	0.007068	1.80E-01	7.87E-02	325.73	
631	Delrin	200	0.0792	51.6	241.8	4.585	2.064	0.008875	2.01E-01	8.82E-02	364.73	
632	Delrin	200	0.0804	51.8	245.2	4.604	2.081	0.008947	2.02E-01	8.86E-02	361.11	43
640	Delrin	400	0.0807	60.0	245.9	5.331	2.790	0.011995	2.34E-01	1.03E-01	416.98	
641	Delrin	400	0.0791	60.6	241.5	5.385	2.847	0.012240	2.36E-01	1.04E-01	428.95	
642	Delrin	400	0.0804	59.8	245.0	5.311	2.769	0.011907	2.33E-01	1.02E-01	416.98	47.5
651	Delrin	600	0.0807	64.2	245.9	5.703	3.192	0.013725	2.50E-01	1.10E-01	446.13	
652	Delrin	600	0.0796	67.0	242.7	5.957	3.483	0.014976	2.61E-01	1.15E-01	472.04	
653	Delrin	600	0.0798	64.5	243.5	5.728	3.220	0.013845	2.51E-01	1.10E-01	452.50	44.9
660	Delrin	800	0.0796	68.2	242.9	6.058	3.601	0.015485	2.66E-01	1.17E-01	479.66	
661	Delrin	800	0.0816	71.0	248.6	6.308	3.906	0.016793	2.77E-01	1.21E-01	488.05	
662	Delrin	800	0.0801	70.1	244.3	6.226	3.804	0.016356	2.73E-01	1.20E-01	490.05	47.4
670	Delrin	970	0.0811	72.4	247.2	6.432	4.060	0.017457	2.82E-01	1.24E-01	500.50	
671	Delrin	970	0.0811	74.9	247.1	6.654	4.345	0.018684	2.92E-01	1.28E-01	517.91	
672	Delrin	970	0.0806	72.0	245.6	6.396	4.014	0.017260	2.81E-01	1.23E-01	500.87	47.2
701	Delrin	0	0.0859	33.7	260.5	2.991	0.879	0.003779	1.31E-01	5.76E-02	220.97	
710	Delrin	0	0.0841	31.3	255.6	2.777	0.758	0.003257	1.22E-01	5.34E-02	209.04	
711	Delrin	0	0.0850	33.0	257.9	2.934	0.845	0.003634	1.29E-01	5.64E-02	218.82	
712	Delrin	0	0.0853	32.5	258.9	2.883	0.816	0.003510	1.27E-01	5.55E-02	214.25	67.6
720	Delrin	50	0.0846	27.4	257.0	2.432	0.581	0.002499	1.07E-01	4.68E-02	182.14	
721	Delrin	50	0.0851	33.7	258.4	2.994	0.880	0.003785	1.31E-01	5.76E-02	222.89	
722	Delrin	50	0.0850	31.2	258.0	2.772	0.755	0.003245	1.22E-01	5.33E-02	206.67	38.9
730	Delrin, N2	960	0.0851	53.7	258.3	4.767	2.231	0.009594	2.09E-01	9.17E-02	355.00	

#	Comment	Press. (mbar)	Energy (V)	Displacement (mm)	Laser Energy (J)	Angle (°)	Height (mm)	Energy (J)	Velocity (m/s)	Impulse (N*s)	Coupling (N/MW)	Mass loss (mg)
731	Delrin, N2	960	0.0844	55.5	256.4	4.930	2.386	0.010259	2.16E-01	9.48E-02	369.87	
732	Delrin, N2	960	0.0834	54.3	253.6	4.825	2.286	0.009828	2.12E-01	9.28E-02	366.00	43.8
740	Delrin, N2	800	0.0876	53.0	265.2	4.708	2.176	0.009356	2.07E-01	9.06E-02	341.42	
741	Delrin, N2	800	0.0847	56.6	257.2	5.027	2.481	0.010667	2.21E-01	9.67E-02	375.99	
742	Delrin, N2	800	0.0857	56.4	260.1	5.014	2.468	0.010614	2.20E-01	9.65E-02	370.82	44
750	Delrin, N2	600	0.0854	54.4	259.1	4.836	2.296	0.009871	2.12E-01	9.30E-02	359.08	
751	Delrin, N2	600	0.0844	61.4	256.2	5.452	2.918	0.012545	2.39E-01	1.05E-01	409.27	
752	Delrin, N2	600	0.0862	62.4	261.5	5.544	3.017	0.012974	2.43E-01	1.07E-01	407.85	76.1
760	Delrin, N2	400	0.0865	53.4	262.2	4.740	2.206	0.009487	2.08E-01	9.12E-02	347.79	
761	Delrin, N2	400	0.0840	54.8	255.3	4.865	2.324	0.009991	2.14E-01	9.36E-02	366.60	
762	Delrin, N2	400	0.0838	70.1	254.7	6.233	3.813	0.016393	2.74E-01	1.20E-01	470.62	50.3
770	Delrin, N2	200	0.0878	40.4	265.8	3.588	1.264	0.005435	1.57E-01	6.90E-02	259.68	
771	Delrin, N2	200	0.0843	47.2	256.2	4.194	1.727	0.007426	1.84E-01	8.07E-02	314.94	
772	Delrin, N2	200	0.0850	47.1	258.0	4.188	1.723	0.007407	1.84E-01	8.06E-02	312.33	38.8
800	Delrin, N2	100	0.0814	36.9	248.0	3.275	1.053	0.004529	1.44E-01	6.30E-02	254.08	
801	Delrin, N2	100	0.0809	40.1	246.7	3.564	1.247	0.005362	1.56E-01	6.86E-02	277.97	
802	Delrin, N2	100	0.0809	39.9	246.7	3.548	1.237	0.005317	1.56E-01	6.83E-02	276.79	36.6
810	Delrin	0	0.0812	37.1	247.2	3.297	1.068	0.004590	1.45E-01	6.34E-02	256.56	
811	Delrin	0	0.0813	35.9	247.7	3.193	1.001	0.004305	1.40E-01	6.14E-02	248.02	
812	Delrin	0	0.0813	33.4	247.6	2.967	0.865	0.003718	1.30E-01	5.71E-02	230.60	68.6
820	Delrin	0	0.0853	33.4	258.8	2.965	0.864	0.003714	1.30E-01	5.71E-02	220.44	
821	Delrin	0	0.0823	32.8	250.5	2.911	0.832	0.003579	1.28E-01	5.60E-02	223.65	
822	Delrin	0	0.0878	33.1	265.9	2.942	0.850	0.003656	1.29E-01	5.66E-02	212.95	66.4
830	Delrin	0	0.0703	34.4	216.5	3.060	0.919	0.003953	1.34E-01	5.89E-02	271.97	

#	Comment	Press. (mbar)	Energy (V)	Displace-ment (mm)	Laser Energy (J)	Angle (°)	Height (mm)	Energy (J)	Velocity (m/s)	Impulse (N*s)	Coupling (N/MW)	Mass loss (mg)
831	Delrin	0	0.0686	32.5	211.4	2.889	0.820	0.003525	1.27E-01	5.56E-02	262.97	
832	Delrin	0	0.0694	32.4	213.7	2.882	0.816	0.003508	1.27E-01	5.55E-02	259.46	68.4
840	Delrin	0	0.0609	32.6	189.1	2.898	0.825	0.003547	1.27E-01	5.58E-02	294.88	
841	Delrin	0	0.0614	32.2	190.3	2.856	0.801	0.003445	1.25E-01	5.50E-02	288.71	
842	Delrin	0	0.0607	31.0	188.4	2.754	0.745	0.003203	1.21E-01	5.30E-02	281.28	67.6
850	Delrin	0	0.0509	31.9	159.5	2.834	0.789	0.003392	1.24E-01	5.45E-02	341.89	
851	Delrin	0	0.0501	31.1	157.0	2.764	0.750	0.003226	1.21E-01	5.32E-02	338.63	
852	Delrin	0	0.0509	29.4	159.4	2.608	0.668	0.002873	1.15E-01	5.02E-02	314.78	67.2
860	Delrin	0	0.0388	25.7	122.9	2.281	0.511	0.002198	1.00E-01	4.39E-02	357.03	
861	Delrin	0	0.0381	25.4	120.7	2.259	0.501	0.002155	9.92E-02	4.35E-02	360.09	
862	Delrin	0	0.0380	26.2	120.4	2.331	0.534	0.002295	1.02E-01	4.49E-02	372.50	59.2
900	Delrin	960	0.0400	44.6	126.4	3.965	1.544	0.006639	1.74E-01	7.63E-02	603.55	
901	Delrin	960	0.0397	44.9	125.6	3.989	1.563	0.006720	1.75E-01	7.67E-02	611.18	
902	Delrin	960	0.0396	43.6	125.3	3.876	1.476	0.006345	1.70E-01	7.46E-02	595.05	56.8
910	Delrin	960	0.0524	56.8	163.9	5.045	2.499	0.010746	2.21E-01	9.71E-02	592.14	
911	Delrin	960	0.0528	57.6	165.2	5.117	2.570	0.011051	2.25E-01	9.84E-02	595.94	
912	Delrin	960	0.0524	56.6	164.0	5.029	2.483	0.010678	2.21E-01	9.67E-02	590.05	54.5
920	Delrin	960	0.0615	57.8	190.9	5.133	2.587	0.011124	2.25E-01	9.87E-02	517.34	
921	Delrin	960	0.0613	63.8	190.2	5.667	3.152	0.013555	2.49E-01	1.09E-01	573.18	
922	Delrin	960	0.0611	62.2	189.6	5.527	2.999	0.012895	2.43E-01	1.06E-01	560.88	46.9
930	Delrin	960	0.0712	64.2	218.8	5.709	3.199	0.013755	2.51E-01	1.10E-01	501.76	
931	Delrin	960	0.0697	67.8	214.5	6.025	3.563	0.015322	2.64E-01	1.16E-01	540.37	
932	Delrin	960	0.0701	67.3	215.9	5.979	3.509	0.015088	2.62E-01	1.15E-01	532.72	44
940	Delrin	960	0.0828	68.0	252.0	6.039	3.579	0.015390	2.65E-01	1.16E-01	460.91	

#	Comment	Press. (mbar)	Energy (V)	Displacement (mm)	Laser Energy (J)	Angle (°)	Height (mm)	Energy (J)	Velocity (m/s)	Impulse (N*s)	Coupling (N/MW)	Mass loss (mg)
941	Delrin	960	0.0825	72.4	251.0	6.432	4.060	0.017457	2.82E-01	1.24E-01	492.76	
942	Delrin	960	0.0807	71.1	246.1	6.320	3.920	0.016854	2.77E-01	1.22E-01	493.93	41.7
950	Delrin	960	0.0836	68.2	254.1	6.058	3.602	0.015489	2.66E-01	1.17E-01	458.53	
951	Delrin	960	0.0817	72.0	248.9	6.400	4.020	0.017284	2.81E-01	1.23E-01	494.58	
952	Delrin	960	0.0824	71.3	250.8	6.332	3.935	0.016921	2.78E-01	1.22E-01	485.68	42.2
1201		0	0.0791	40.4	241.5	3.588	1.264	0.005435	1.57E-01	6.90E-02	285.76	
1202		0	0.0793	47.1	242.1	4.187	1.721	0.007401	1.84E-01	8.05E-02	332.76	
1203		0	0.0787	52.2	240.2	4.636	2.111	0.009075	2.03E-01	8.92E-02	371.35	
1204		0	0.0779	45.8	238.2	4.073	1.629	0.007004	1.79E-01	7.84E-02	328.99	
1205		0	0.0787	2.8	240.4	0.253	0.006	0.000027	1.11E-02	4.86E-03	20.22	
1210		0	0.0791	10.2	241.3	0.902	0.080	0.000343	3.96E-02	1.73E-02	71.90	
1211		0	0.0772	16.7	236.2	1.486	0.217	0.000933	6.52E-02	2.86E-02	121.09	
1212		0	0.0784	15.7	239.5	1.390	0.190	0.000816	6.10E-02	2.68E-02	111.71	28.4
1300		0	0.0797	10.0	243.1	0.888	0.078	0.000333	3.90E-02	1.71E-02	70.31	
1301		0	0.0802	11.8	244.6	1.046	0.108	0.000463	4.59E-02	2.01E-02	82.31	
1302		0	0.0797	11.5	243.1	1.021	0.102	0.000440	4.48E-02	1.96E-02	80.78	18.1
1400		0	0.0807	49.0	246.0	4.350	1.858	0.007990	1.91E-01	8.37E-02	340.23	
1401		0	0.0790	52.5	241.1	4.665	2.137	0.009187	2.05E-01	8.97E-02	372.14	
1402		0	0.0798	53.8	243.3	4.776	2.240	0.009630	2.10E-01	9.19E-02	377.64	113.3
1410		0	0.0821	52.5	249.9	4.663	2.135	0.009180	2.05E-01	8.97E-02	358.90	
1411		0	0.0792	50.2	241.8	4.464	1.957	0.008413	1.96E-01	8.59E-02	355.12	
1412		0	0.0736	51.1	225.9	4.542	2.026	0.008710	1.99E-01	8.74E-02	386.82	112.6
1420		0	0.0701	45.3	215.8	4.020	1.587	0.006825	1.76E-01	7.73E-02	358.38	
1421		0	0.0684	46.4	210.8	4.119	1.666	0.007164	1.81E-01	7.92E-02	375.92	
1422		0	0.0687	48.2	211.8	4.279	1.798	0.007731	1.88E-01	8.23E-02	388.75	104.3

#	Comment	Press. (mbar)	Energy (V)	Displace-ment (mm)	Laser Energy (J)	Angle (°)	Height (mm)	Energy (J)	Velocity (m/s)	Impulse (N*s)	Coupling (N/MW)	Mass loss (mg)
1430		0	0.0591	41.4	183.7	3.678	1.329	0.005713	1.61E-01	7.08E-02	385.20	
1431		0	0.0604	42.6	187.4	3.788	1.409	0.006057	1.66E-01	7.29E-02	388.74	
1432		0	0.0592	42.4	184.1	3.765	1.392	0.005986	1.65E-01	7.24E-02	393.43	94.2
1440		0	0.0504	35.5	157.8	3.157	0.979	0.004208	1.39E-01	6.07E-02	384.83	
1441		0	0.0502	36.0	157.4	3.197	1.004	0.004317	1.40E-01	6.15E-02	390.85	
1442		0	0.0498	36.2	156.2	3.219	1.018	0.004375	1.41E-01	6.19E-02	396.40	82.3
1450		0	0.0383	28.1	121.3	2.497	0.613	0.002634	1.10E-01	4.80E-02	396.03	
1451		0	0.0386	28.2	122.2	2.501	0.614	0.002641	1.10E-01	4.81E-02	393.82	
1452		0	0.0380	28.1	120.3	2.496	0.612	0.002632	1.10E-01	4.80E-02	399.11	66.8

This Page Intentionally Left Blank

Table B – US Lightcraft

Stable resonator

Total pendulum mass: 494.0 g

Pendulum length (center of mass): 645 mm

#	Comment	Press. (mbar)	Energy (V)	Displace-ment (mm)	Laser Energy (J)	Angle (°)	Height (mm)	Energy (J)	Velocity (m/s)	Impulse (N*s)	Coupling (N/MW)	Mass loss (mg)
1000	Delrin	0	0.0842	39.7	255.8	3.526	1.221	0.005918	1.55E-01	7.65E-02	298.94	
1001	Delrin	0	0.0771	38.5	235.9	3.423	1.151	0.005577	1.50E-01	7.42E-02	314.71	
1002	Delrin	0	0.0779	38.5	238.2	3.418	1.147	0.005560	1.50E-01	7.41E-02	311.18	154.9
1010	Delrin	0	0.0776	37.8	237.3	3.357	1.106	0.005362	1.47E-01	7.28E-02	306.70	
1011	Delrin	0	0.0770	37.6	235.4	3.339	1.095	0.005305	1.47E-01	7.24E-02	307.54	
1012	Delrin	0	0.0779	38.7	238.1	3.438	1.161	0.005626	1.51E-01	7.46E-02	313.19	148.4
1020	Delrin	0	0.0671	32.3	207.2	2.867	0.807	0.003912	1.26E-01	6.22E-02	300.07	
1021	Delrin	0	0.0673	33.5	207.7	2.974	0.869	0.004211	1.31E-01	6.45E-02	310.54	
1022	Delrin	0	0.0666	33.0	205.7	2.930	0.843	0.004086	1.29E-01	6.35E-02	308.92	131.4
1030	Delrin	0	0.0580	28.1	180.4	2.492	0.610	0.002956	1.09E-01	5.40E-02	299.58	
1031	Delrin	0	0.0586	28.4	182.3	2.521	0.624	0.003026	1.11E-01	5.47E-02	299.97	
1032	Delrin	0	0.0583	28.4	181.5	2.527	0.627	0.003039	1.11E-01	5.48E-02	301.87	115.2
1040	Delrin	0	0.0493	23.1	154.6	2.048	0.412	0.001996	8.99E-02	4.44E-02	287.33	
1041	Delrin	0	0.0503	23.2	157.5	2.059	0.417	0.002019	9.04E-02	4.47E-02	283.51	
1042	Delrin	0	0.0492	23.0	154.2	2.045	0.411	0.001991	8.98E-02	4.43E-02	287.63	98.1
1050	Delrin	0	0.0375	16.4	119.0	1.458	0.209	0.001012	6.40E-02	3.16E-02	265.67	
1051	Delrin	0	0.0380	17.1	120.3	1.515	0.226	0.001093	6.65E-02	3.29E-02	273.10	
1052	Delrin	0	0.0382	17.4	120.9	1.542	0.234	0.001132	6.77E-02	3.34E-02	276.64	75.1
1060	Delrin	50	0.0775	36.4	236.9	3.235	1.028	0.004980	1.42E-01	7.01E-02	296.14	
1061	Delrin	50	0.0758	35.9	232.1	3.189	0.999	0.004842	1.40E-01	6.92E-02	297.93	
1062	Delrin	50	0.0775	36.2	236.9	3.215	1.015	0.004920	1.41E-01	6.97E-02	294.35	146.6
1070	Delrin	100	0.0774	38.1	236.5	3.388	1.128	0.005465	1.49E-01	7.35E-02	310.70	
1071	Delrin	100	0.0777	38.0	237.4	3.380	1.122	0.005436	1.48E-01	7.33E-02	308.73	
1072	Delrin	100	0.0777	38.0	237.5	3.372	1.116	0.005410	1.48E-01	7.31E-02	307.78	149.2

#	Comment	Press. (mbar)	Energy (V)	Displacement (mm)	Laser Energy (J)	Angle (°)	Height (mm)	Energy (J)	Velocity (m/s)	Impulse (N*s)	Coupling (N/MW)	Mass loss (mg)
1080	Delrin	150	0.0789	38.4	240.8	3.408	1.141	0.005528	1.50E-01	7.39E-02	306.90	
1081	Delrin	150	0.0780	39.0	238.5	3.465	1.179	0.005714	1.52E-01	7.51E-02	315.09	
1082	Delrin	150	0.0774	38.7	236.5	3.440	1.162	0.005632	1.51E-01	7.46E-02	315.42	146.5
1090	Delrin	200	0.0782	39.3	239.0	3.487	1.194	0.005787	1.53E-01	7.56E-02	316.44	
1091	Delrin	200	0.0780	38.9	238.2	3.460	1.175	0.005696	1.52E-01	7.50E-02	314.91	
1092	Delrin	200	0.0777	39.5	237.6	3.505	1.206	0.005847	1.54E-01	7.60E-02	319.87	146.8
1100	Delrin	300	0.0780	40.5	238.4	3.602	1.274	0.006174	1.58E-01	7.81E-02	327.62	
1101	Delrin	300	0.0772	41.1	236.1	3.647	1.306	0.006330	1.60E-01	7.91E-02	334.97	
1102	Delrin	300	0.0762	40.5	233.1	3.599	1.272	0.006165	1.58E-01	7.80E-02	334.83	147.6
1110	Delrin	400	0.0783	42.1	239.1	3.741	1.375	0.006662	1.64E-01	8.11E-02	339.25	
1111	Delrin	400	0.0787	42.9	240.4	3.808	1.424	0.006901	1.67E-01	8.26E-02	343.47	
1112	Delrin	400	0.0789	43.9	240.9	3.900	1.493	0.007237	1.71E-01	8.46E-02	351.06	150.6
1120	Delrin	600	0.0775	42.4	237.0	3.767	1.394	0.006754	1.65E-01	8.17E-02	344.70	
1121	Delrin	600	0.0775	42.3	236.9	3.761	1.389	0.006731	1.65E-01	8.16E-02	344.29	
1122	Delrin	600	0.0779	42.5	238.1	3.774	1.399	0.006779	1.66E-01	8.18E-02	343.70	148.1
1130	Delrin	800	0.0778	42.6	237.8	3.788	1.409	0.006830	1.66E-01	8.21E-02	345.41	
1131	Delrin	800	0.0776	42.6	237.3	3.780	1.403	0.006802	1.66E-01	8.20E-02	345.50	
1132	Delrin	800	0.0783	42.8	239.1	3.801	1.419	0.006875	1.67E-01	8.24E-02	344.73	149.3
1140	Delrin	980	0.0771	41.9	235.7	3.718	1.358	0.006580	1.63E-01	8.06E-02	342.07	
1141	Delrin	980	0.0786	43.1	239.9	3.827	1.438	0.006969	1.68E-01	8.30E-02	345.84	
1142	Delrin	980	0.0791	44.2	241.4	3.929	1.516	0.007346	1.72E-01	8.52E-02	352.95	149.4
1150	Delrin, N2	980	0.0790	35.6	241.1	3.165	0.984	0.004769	1.39E-01	6.86E-02	284.72	
1151	Delrin, N2	980	0.0784	35.8	239.6	3.183	0.995	0.004823	1.40E-01	6.90E-02	288.11	
1152	Delrin, N2	980	0.0775	34.8	236.8	3.087	0.936	0.004536	1.36E-01	6.69E-02	282.71	147.6

AFRL-PR-ED-TR-2002-0044
Primary Distribution of this Report:

AFRL/PRSP   (15 CD)
Dr. Frank Mead
10 E. Saturn Blvd
Edwards AFB CA 93524-7680

Dr. Harold Ackerman (1 CD)
AFRL/DEL
Bldg. 499
Kirtland AFB, NM 87117

Ranney G. Adams (1 HC)
AFRL/PROI (Public Affairs)
2 Draco Drive
Edwards AFB CA 93524-7808

AFRL/PR Technical Library (2 CD + 1 HC)
6 Draco Drive
Edwards AFB CA 93524-7130

Chemical Propulsion Information Agency (1 CD)
Attn: Tech Lib (Dottie Becker)
10630 Little Patuxent Parkway, Suite 202
Columbia MD 21044-3200

Defense Technical Information Center
(1 Electronic Submission via STINT)
Attn: DTIC-ACQS (Acquisitions)
8725 John J. Kingman Road, Suite 94
Ft. Belvoir VA 22060-6218

Chris Beairsto (1 CD)
Directorate for Applied Technology
  Test and Simulation
STEWS-DATTS-OO
WSMR NM 88002

Dr. Greg Benford (1 CD)
Physics Department
University of California
Irvine, CA 92717

Dr. Jim Benford (1 CD)
Microwave Sciences, Inc.
1041 Los Arabis Ln.
Lafayette, CA 94549

Dr. Gary L. Bennett (1 CD)
7517 West Devonwood Dr.
Boise, ID 83703

Dr. Mitat Birkan (1 CD)
AFOSR/NA
801 N. Randolf St.
Arlington, VA 22203

Dr. Jon Campbell (1 CD)
P.O. Box 295
Harvest, AL 35749

Dr. Phil Carpenter (1 CD)
US Dept. of Energy
Oak Ridge National Laboratory
P.O. Box 2008, MS: 6269
Oak Ridge, TN 37831

Dr. Pat Carrick (1 CD)
1500 Wilson Blvd.
Arlington, VA 22304

Dr. David Chenault (1 CD)
SY Technology, Inc
654 Discovery Dr.
Huntsville, AL 35802

Mr. John Cole (1 CD)
NASA/Marshall Space Flight Center
TD-15
Bldg. 4203, Rm 4401
Marshall Space Flight Center, AL 35812

Dr. Jim Degnan
PL/WSP
Kirtland AFB, NM 87117

Dr. Ingrid Wysong (1 CD)
EOARD (Box 14)
223-321-Old Merylebone Rd.
London NW1 5th
United Kingdom/FPO New York, NY 09510

Dr. Robert Frisbee (1 CD)
JPL, MS 125-109
4800 Oak Grove Dr.
Pasadena, CA 91109

Dave Froning (1 CD)
Flight Unlimited
5450 Country Club
Flagstaff, AZ 86004

Mr. Bob Geisler (1 CD)
20333 Old Town Rd.
Tehachapi, CA 93561

Dr. Kenneth Goretta (5 CD)
AOARD
Tokyo, Japan

Clark W. Hawk, Director (1 CD)
Propulsion Research Center
University of Alabama in Huntsville
5000 Technology Drive, TH S-266
Huntsville, AL 35899

Lt. Col. Ryan K. Haaland (1 CD)
USAFA/DFP
Colorado Springs, CO 80916

Dr. Victor Hasson
Trex Enterprises , Inc.
10455 Pacific Center Ct.
San Diego, CA 92121

Mike Kaiserman (1 CD)
Raytheon Missile Systems Company
Bldg 805, M/S C3
Tucson, AZ 85734

Dr. Jordon Kare (1 CD)
222 Canyon Lakes Pl.
San Ramon, CA 94583

Dr. Dennis Keefer (1 CD)
The University of Tennessee Space
  Institute
Tullahoma, TN 37388

Mr. Sandy Kirkindall (1 CD)
NASA/MSFC, TD40
Bldg. 4203, Room 2160
Huntsville, AL 35812

Dr. Timothy Knowles (1 CD)
ESLI
6888 Nancy Ridge Dr.
San Diego, CA 92121

AFRL/PRSP   (1 CD)
Sean Knecht
10 E. Saturn Blvd
Edwards AFB CA 93524-7680

AFRL/PRSP   (1 CD)
Dr. Carl W, Larson
10 E. Saturn Blvd
Edwards AFB CA 93524-7680

Dr. Sheldon Meth (1 CD)
DARPA
Tactical Technology Office
3701 N. Fairfax Dr.
Arlington, VA 22203

Dr. Michael M. Micci (1 CD)
Prof. of Aerospace Engineering
233 E. Hammond Bldg.
University Park, PA 16802

Dr. George Miley (1 CD)
University of Illinois, Dept. of Nuclear Engr.
214 Nuclear Engineering Laboratory
103 South Goodwin Ave.
Urbana, IL 61801

Dr. Marc Millis (1 CD)
NASA Glenn Research Center
M.S. SPTD-2
21000 Brookpark Road, MS: 86-2
Cleveland, OH 44135

Dr. Aurthur Morrish (1 CD)
DARPA/ATO
3701 N. Fairfax Dr.
Arlington, VA 22203

Dr. Paul Murad (1 CD)
Sr. Analyst, Director for Intel Production
Missile & Space Intel Center
Defense Intelligence Agency
Washington, DC 20340-6054

Dr. Don Messitt
902 Dianthus Lane
El Dorado Hills, CA 95762

Dr. Alan Pike (1 CD)
DSAS
1988 Crescent Park Drive
Reston, VA 20190

Dr. Andrew W. Pakhomov (1 CD)
Dept. of Physics
University of Alabama in Huntsville
Huntsville, AL 35899

Ben Plenge (1 CD)
101 W. Eglin Blvd
Suite 342
Eglin AFB, FL 32542-6810

Dr. Claude Phipps (1 CD)
200A Ojo de la Vaca Rd.
Santa Fe, NM 87505

Dr. James P. Riley (1 CD)
Northeast Science & Technology, Inc.
117 North Shore Blvd.
Cape Cod, MA 02537

Dr. Eric E. Rice (1 CD)
Orbital Technologies Corp.
402 Gammon Place, Suite 10
Madison, WI 53719

Mr. Wolfgang Schall (10 CD)
DLR/Institute for Technical Physics - Vaihingen
Pfaffenwaldring 38-40
D-70569 Stuttgart
Germany

Steve Squires (1 CD)
Directorate of Applied Technology
   Test and Simulation
STEWS-DATTS-OO
WSMR, NM 88002

Dr. Uchida Shigeaki (10 CD)
Institute for Laser Technology-Osaka University
2-6 yamada oka
Suita, Osaka 565-0871
Japan

Dr. Kenneth D. Ware (1 CD)
Defense Nuclear Agency
Simulation Technology
6801 Telegraph Road
Alexandria, VA 22310

Dr. Feiedwardt Winterberg (1 CD)
University of Nevada
Desert Research Institute
Reno, NV 89507

Dr. John Staiger (1 CD)
AFRL/VAAI
Wright Patterson AFB, OH 45433

Dr. Thomas M York (1 CD)
1215 Inverary Pl.
State College, PA 16801

Dr. Charles Suchomel (1 CD)
AFRL/VAAA
Wright Patterson AFB, OH 45433

Dr. Victor F. Tarasenko (5 CD)
Head of Laboratory of Optical Radiation
4, Akademichesky Ave.
Tomsk, 634055
Russia

Ms Shelley Thomson (1 CD)
P.O. Box 82575
Albuquerque, NM 87198

Ms Charlotte Thorton (1 CD)
Mechanical Engineering
P.O. Box 20465
Stanford, CA 94309

Dr. Ten-See Wang (1 CD)
NASA/MFSC, TD64
Huntsville, AL 35812

Dr. Victor V. Apollonov (5 CD)
General Physics Institute RAS & JSC
"Energomashtechnika
Vavilov St. 38. 117942
Moscow, Russia